BIODEGRADABLE COMPOSITE MATERIALS – ARBOFORM: A REVIEW

Simona Plăvănescu (Mazurchevici)

"Gheorghe Asachi" Technical University of Iasi, Romania, Blvd. Mangeron, No. 59A, 700050 Iasi, Romania

Corresponding author: Simona Plăvănescu (Mazurchevici), simona0nikoleta@yahoo.com

Abstract: Large-scale use of non-renewable resources has led to a significant increase of both the fossil raw materials pricing - a threat to the global economy and the last two decades atmospheric concentration of carbon dioxide – known to affect the global climate. Estimates on the following decades indicate these resources are to be exhausted. Therefore a considerable lowering of the finite resources consumption would prevent the needs of the present from compromising the ability of future generations to meet their own needs. It is known the most of the energy resources, the polymers, and the synthetic organic polymers are derived from fossil fuels such as oil and natural gas. Resources can be maintained if a sustainable future is to be provided by using bio-based materials comprising maximum possible quantity of biomass renewable derivatives. Bioplastics, biofibers, biocomposites and related biomaterials will serve as substitutes for materials and products traditionally made from petroleum resources. To anticipate this need, the German FraunhoferInstitute for Chemical Technologytogether with Tecnaro GmbH Company (founded byJurgenPfitzer and Helmut Nagele) have made studies and developed - based on wood components - a new material which can be processed in the same way as thermoplastics. Arboform is the output of natural fibres, lignin, and additives mixing. It can be obtained by using different types of lignin (30%) extracted out of processes and sources (10 types at least), natural fibres 60% (flax, hemp, sisal, wood) and10% natural additives (softeners, pigments, processing agents, etc.). Arboform is the trade name for a fully biodegradable bioplastic composite also known as "liquid wood". The material properties – biodegradability and reusability up to ten times without modifications of its features - recommended it to be the near future alternative to all plastic materials. Depending on the quantity of the mixed components, Arboform can be provided in three different variants: LV3 Nature, F45Nature and LV5 Nature. The component elements are mixed and tamped without heating so that to obtain compound granules. This composite material can be injected into moulds by the same injection technology applied to plastics. Arboform is used in the manufacture of a wide range of products, for example: automotive parts, modular circuit boards, watch cases, computer and television set components, etc.
In terms of biodegradation, Arboform behaves like wood as it decomposes into water, humus and carbon dioxide proving it to be more eco-friendly than plastics emitting fumes when incinerated. Moreover, Arboform production does not involve supplementary cutting down of trees as lignin is a pulp and paper industry product.
Arboform is a high-quality thermoplastic engineering material and is involved in applications requiring state-of-art technology standards. Natural wood positive properties joining the processing features of thermal plastic materials make Arboform the "liquid wood" capable to replace in future times any regular plastic within all activity fields.
The hereby study describes the lignin production process, biodegradability against international standard ISO 1485: 2004, Arboform processing, mechanical, electrical and thermal properties of samples, and the microstructural analysis.
Key words: production, development, biodegradability, properties, applications.

1. INTRODUCTION

Human society has used and continues to widely use plastic materials due to the extensive versatility, cost-effective prices and manufacturing process. Almost all synthetic plastics are obtained out of petroleum and its components. Moreover, most of the plastic materials derived from fossil resources are not biodegradable. Large utilization of plastics and other materials have led over the years to an increase of plastic wastes which are frequently considered to be municipal solid wastes [1].
The main objectives of current fabrication and future development activities consider the following [2]:
• Composite materials obtained from natural resources;
• Plastic properties: the materials and component parts of the injected product are required to be provided with the plastic material properties verified against the standard feature test procedures;
• Use of standard processing technologies and equipment adjusted by small modifications on injection mouldings;
• Identification of technical advantages: the materials can be used to obtain high-quality thermoplastics reinforced with natural fibres for applications within consumer products industry, electronics industry, automotive industry, etc.;
• Energy conservation: injection at low temperatures

(< 160°C), thermal stability at 95°C at least or even 105°C [2].

Lignin is a natural polymer and main component of biomass, with content in trees and other woody-plants up to 30% and represents the starting point for a new class of thermoplastics made of renewable resources [1]. The growing interest in green ecology and ecological sustainability has also contributed to directing attention to biomass and particularly to lignocelluloses stock as a promising, renewable, and extended resource for biopolymers [3]. Lignocellulosic biomass comprises three main biopolymers: cellulose, hemicelluloses and lignin [4].

Lignin is now considered the main aromatic renewable resource as it is an excellent alternative feedstock for the elaboration of chemicals and polymers. As a highly abundant biopolymeric material, lignin and cellulose represent together one of the major components. Each year, large quantities of lignin are available from numerous pulping processes such as paper and biorefinery industries. The extraction of lignin from lignocellulosic biomass represents the key point to its large use for industrial applications.

Lignin is a major component of woody plants as it provides strength and adequate structure to the cell walls, controls the fluid flow rate, and protects from biochemical stress by enzymatic degradation of other components. [3].

Although the quantity of lignin reaches 50 million tons per year [5] only a small amount up to 2%is recovered and used for a wide range of products or chemical materials such as Arboform [6]. The rest of 98% are used as fuel/ raw material in the paper mills. Nevertheless, there are enough reasons and good arguments to use this promising resource in industry applications [7].

Lignin is formed by photosynthesis, makes up about 15-25% of the substance of every wood or plant, and is the second abundant organic polymer on Earth as shown in Figure 1 [1, 7].

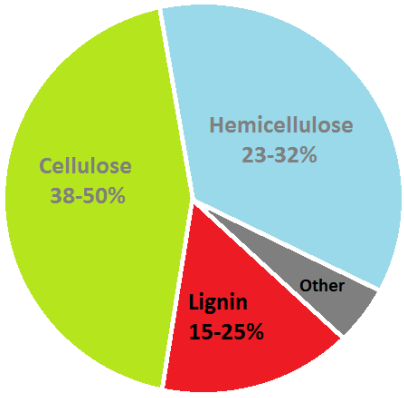

Fig. 1. Simplified structure of wood

Within last years, a number of new initiatives have been performed for a more efficient management of lignin wastes produced by chemical delignification and wood industry. Sulphite substances and the components of these lignosulfonates are the most used wastes derived from paper and cellulose industry [2].

Different types of lignin are available as more than 20 variants are frequently produced. For a lignin-matrix material such as Arboform, the input and lignin quality are highly important [10]. The near infra-red spectroscopy (NIRS) provides online control of thermoplastic processing operations. The NIRS method has been introduced to measure the lignin content [8, 9]. The infra-red spectrum of some types of lignin is indicated in Figure 2. As the differences are not clear in the main band between 1400 and 1500 nm the structure is provided by physical properties, i.e. the particle size.

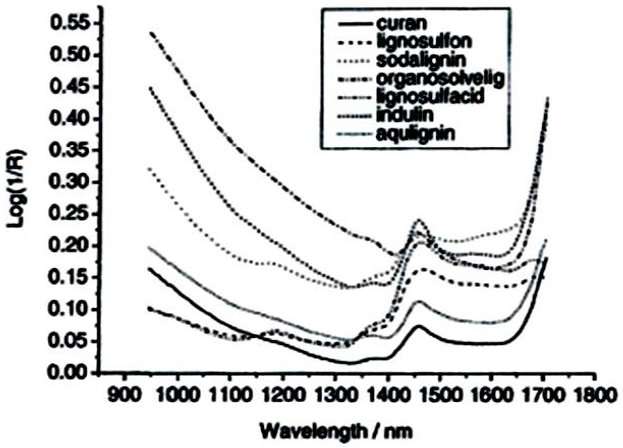

Fig. 2. Different types of NIR spectra, [2]

Following a statistical analysis involving multiple variants [11, 12] of the principal component analyzed (PCA) by NIR, the differences between the studied lignin types graphically represented in Fig.3 can be clearly distinguished.

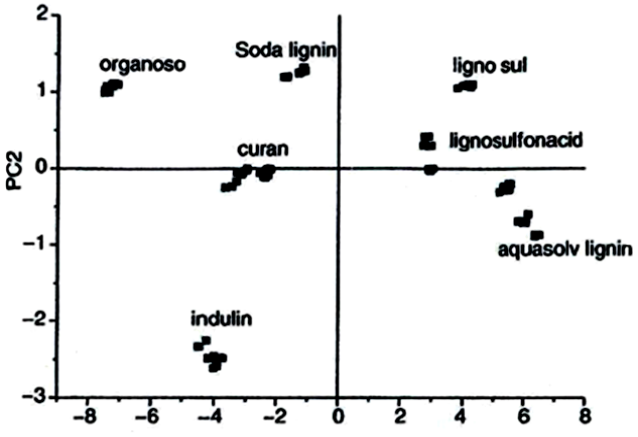

Fig. 3. Main component analysis (PCA), [2]

Lignin has been determined by NIR/IR spectroscopy, thermal analysis methods and scanning electron microscopy (SEM). The IR/ NIR spectra are similar

to the spectra of other lignin types (Fig. 4). Nevertheless, the chemometric analyses (principal components analysis, PCA and partial least squares regression / multiple linear regression, PLS) can clearly indicate the difference between HPH -lignin (high pressure hydrolysis) and other types, as shown in Figure 4.

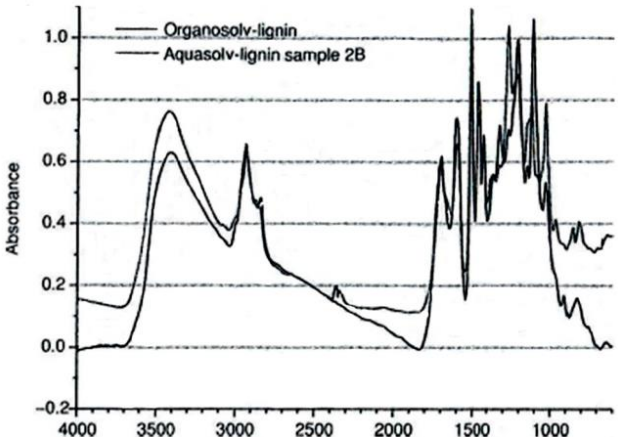

Fig. 4. IR analysis of two samples comparing HPH Aquasolv lignin andOrganosolv lignin, [2]

Figure 5, [14] presents an exhibits the most frequent chemical process used for lignin separation (HPH).

Almost forty years ago, the American scientists have taken the first steps towards stopping the human dependence on plastic products. Tecnaro German company has succeeded in manufacturing a product that looks like wood, has woody-structure, can be moulded/ injected by the same procedure as that of plastic materials, and, in addition to these properties, is biodegradable and known as "liquid wood" 17].

In addition, many residues of agricultural products that are currently unused contain substantial amounts of lignin (Table 1, [13]).

Concerning the natural fibres reinforcing process, the new biofibers and wood fibres could be used (Figure 6, [15, 16]).

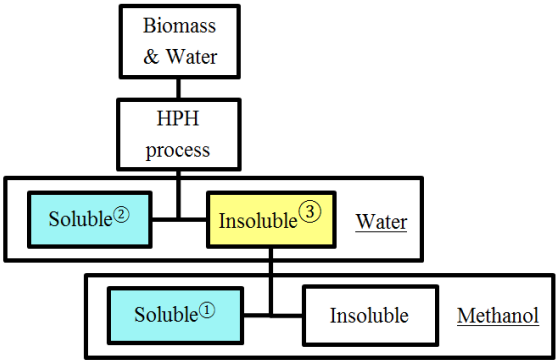

Fig. 5. Lignin separations, [14]

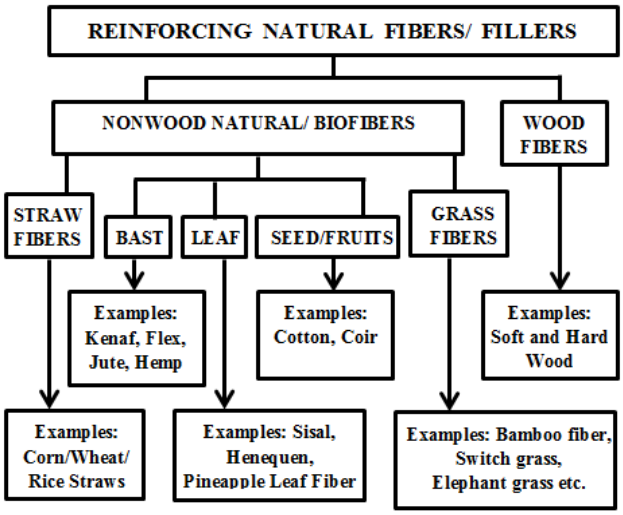

Fig. 6. Reinforcing natural fibers, [15, 16]

Table 1. Content of lignin, hemicelluloses, cellulose, nitrogen and ash from different rests and residues of plants and fruits [2, 13]

	Lignin	Cellulose	Hemi-cellulose	Nitrogen	Ash
Meal from maize (hominy)	2.0	11.0	42.0	1.84	1.0
Malt sprouts hulls	3.0	15.0	28.0	4.5	7.0
Brewers grains, dehydrate	6.0	18.0	22.0	4.16	4.0
Crape stems	12.0	-	-	< 0.5	-
Straw from rice	12.5	32.1	24.0	-	17.5
Coffee ground	15.0	-	9.0	0	2.0
Hay, weathered	15.0	30.0	13.0	1.6	8.0
Straw from Soybean	16.0	38.0	16.0	0.83	6.0
Bamboo	20.1	-	19.6	-	3.3
Hulls from peanuts	23.0	42.0	9.0	1.25	4.0
Cocoa bean	25.0	-	-	2.56	-
Olive waste	28.0	-	-	0	-
Grape pomace	38.0	19.0	1.0	0	10.0
Fruit pits	40.0	-	-	-	-

"Liquid wood" is available in three different versions: ARBOFORM®Liquid wood (based on lignin, organic additives and natural fibers), ARBOBLEND®plastic composite with wood (its content is based on biopolymers degree, e.g.: lignin, starch, natural resins, wax and cellulose), ARBOFILL®biopolymeric composite (polymers and natural fibres-based compound provided with natural cork aspect) [6, 18].

Arboform has been developed some years ago, in 1998, when FraunhoferInstitute for Chemical Technology together with Tecnaro GmbH, Germany have investigated and developed out of wood composing elements a new compound able to be processed like a thermoplastic material. The new product can be manufactured by using multiple types of lignin (30%) from different processes or sources (more than 10 types), 60% organic fibers (flax, hemp, sisal, wood) and 10% organic additives (plasticizers, pigments, processing agents, etc.)[2, 6, 19].Arboform is available in three product variants according to the corresponding quantities of mixed components: LV3 Nature, F45Nature and LV5 Nature [6]. Table 2 bellow indicates the possible composition alternatives [2].

Table 2.Variations in composition, [2]

Matrix		
Lignin	30%	60%
Fibre reinforcement (loose fibres)		
hemp (e.g. H1)	10%	60%
flex (e.g. F4)	10%	60%
Additives		
processing aids (PrAi)	0%	10%
impact modifier	0%	20%
flame retardants	0%	15%

The variations of Arboform composition in what concerns both quality and quantity allow adjustments of strength, rigidity, dimensional stability with varying temperatures and other material properties in order to comply with specific product requirements [20, 21].

Arboform degrades (Figure 7) just like wood, into water, humus, and carbon dioxide, therefore making it more eco-friendly than the fume-emitting burning of plastics [22]. Moreover, because lignin is a by-product of the paper making industry, Arboform production does not require additional cutting down of trees. Every year, the paper and pulp industry alone produces 130 million kg of lignin [24].

Arboform is a high-quality thermoplastic material made exclusively from renewable resources, with no adverse effects on human health.

Researchers have identified no changes of the material mechanical properties, i.e. behaviour in fire and durability, as the material is renewable [24].Arboform behaves like any petrochemical plastic material which means it can be heated and moulded/ injected into a broad range of complex mouldings [25].

Being made one hundred percent from renewable resources, an Arboform product, just like wood-based products, can be disposed by incineration at the end of its useful life. Therefore, the incineration of the product will emit into the atmosphere just the same amount of CO_2 that the plant previously took from the atmosphere while it was growing. So this is a closed CO_2 cycle without any accumulation of CO_2 in atmosphere and, hence, no more adding to the greenhouse effect [26].

The only drawbacks to be considered for liquid wood could be the weight, much higher than of the ordinary plastics, and the production costs, almost double that of the most common plastic, polypropylene.

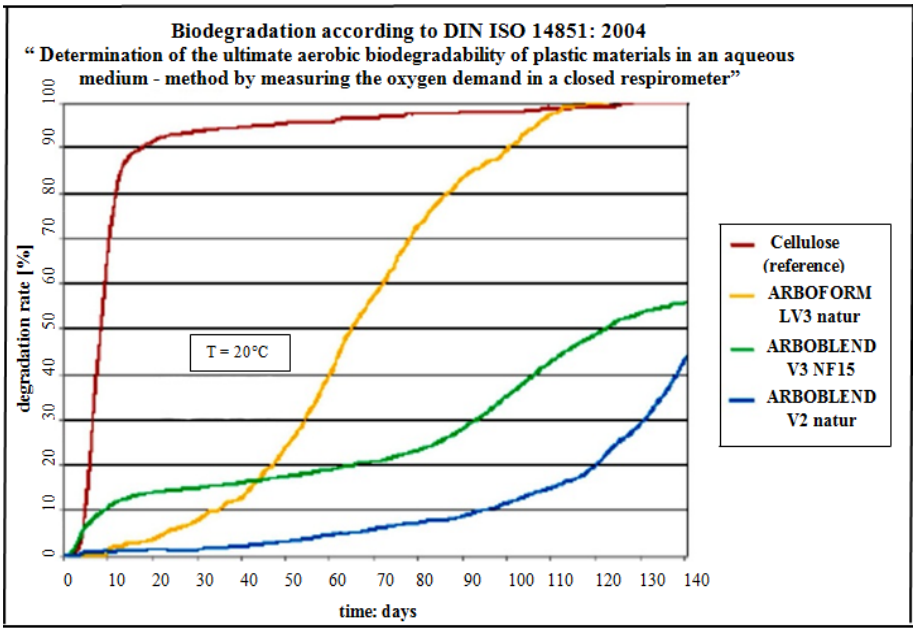

Fig. 7. Biodegradation of "liquid wood" [23]

Arboform has been developed to such level that it can successfully replace plastic. A few of biomass materials are indicated in Figure 8 [2].

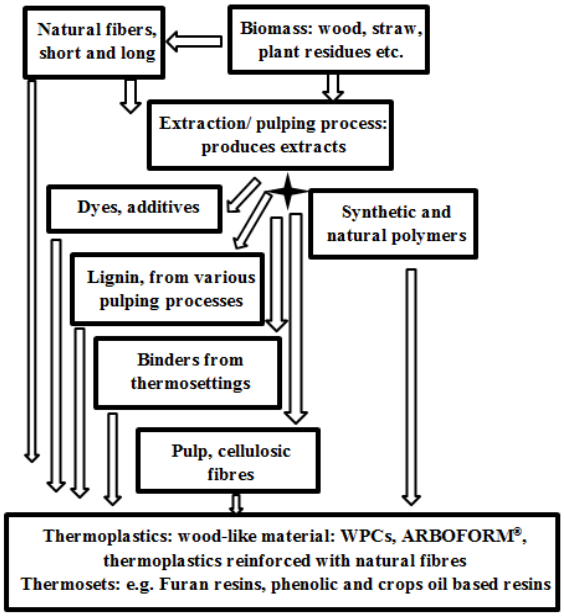

Fig. 8. Plastic–Biomass material [2, 18]

Arboform does not require bonding agents or compatibilizers like the natural bond of lignin as the lignocellulosic fibres are rebounded during processing. Certain combinations of different types of fibres (organic and synthetic) are found to have a positive influence on the properties of the composites. [16].

Figure 9 exhibits tensile strength vs. modulus of elasticity in tension [27] for the 3 types of "liquid wood" (Arboform, Arboblend, Arbofill), as well as for the plastic materials: PS-Polystyrene, ABS-Acrylonitrile butadiene styrene, PP-Polypropyleneand, PLA – Polylactic acid.

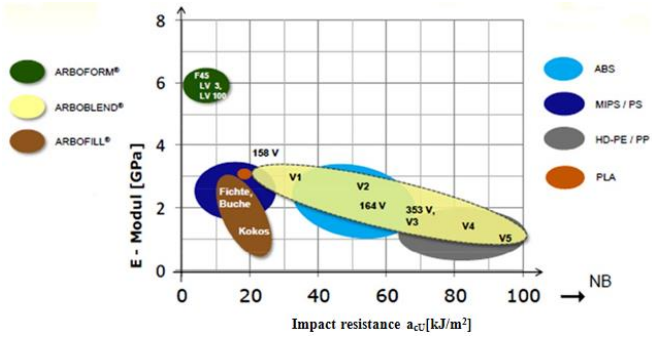

Fig. 9. "Liquid wood" vs.conventional plastic [27]

2. ARBOFORM PROCESSING

Arboform granules can be processed by different procedures, i.e. injection moulding, extrusion, calendering, blow molding, deep drawing or pressing into moulded parts, semi-finished products, sheets, films or profiles. The most frequently used process in order to obtain Arboform-based parts is the injection molding [18].

The injection moulding of Arboform granules can be provided by means of standard injection equipment. The injection temperature varies between 155÷170°C. During the process one of the nozzles is open 2.5 - 4.0mm. The injection pressure must be high enough so that to ensure easy worm gear rotation. The injection pressure should be as high as possible (150 MPa) and so is the injection speed. The holding pressure should be about 30% of the machine capacity and the related time only 0.5÷2 seconds. The cooling time must be about 20% higher than of normal thermal plastic material.

The molding injection devices should be fabricated for serial production of specially selected materials. When the component parts are designed, the instruments/ devices available from plastic components injection of the same parts may be used for a first approach of studies. This operation is frequently providing good results and corresponding quality. Nevertheless, within complex cases, the serial production for development purposes requires new instruments specially adjusted.

The following key issues should be considered:

• Shrinkage in the injection molding process is very low and must not exceed 0.3 %;

• The moulds must be fitted with mould release spring providing quick operating cycles;

• Low shrinkage value of Arboform requires application of not very thin ribs on the moulding plates;

• The heated port of nozzles functions only in limited cases [16].

The general guidelines bellow for an adequate injection moulding processing of Arboform parts should be considered:

• Granules should not be pre-dried, normal storage conditions (dry at temperature 25 °C);

• The injection moulding machine manufacturing temperature is to be achieved by low-melting PE-LD (low-density polyethylene);

• The material must be keptin the injection moulding machine maximum 15 minutes, under manufacturing temperature conditions; in the case of longer dwell time clean intermediately with LD-PE;

• Lignin-compounds must not be maintained in the same place with other hot polymers; cool down immediately, e.g. by using water [2].

According to [17], the Arboform manufacturing process by means of moulding injection can be developed if taking into consideration the two-level input parameters (the 6 parameters listed within Table 3). For study plan purposes the author has used Taguchi method.

The most important effects on the process are provided by the injection pressure, followed by the melting temperature and matrix temperature (Figure 10). The screw displacement, injection time and cooling time have less influence on the injection process.

Table 3.The level values of input parameters

Input parameter levels	melt temperature [°C]	injection time [s]	cooling time [s]	screw displacement [mm]	injection pressure [MPa]	matrix temperature [°C]
First level	165	9	18	60	80	50
Second level	180	11	25	80	100	80

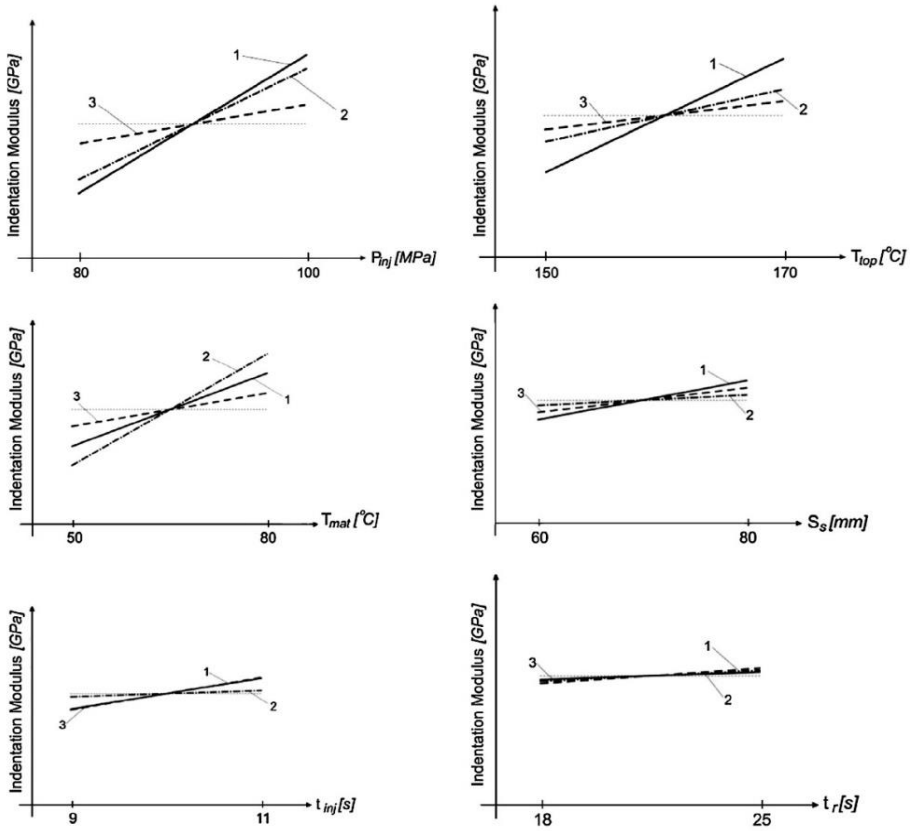

Fig. 10. Input parameters average effects on Indentation Modulus: 1 - Arboform L, V3 Natura; 2 - ArboblendV2 Natura; 3 – Arbofill Fitchie [17]

3. MECHANICAL PROPERTIES

3.1 The Influence of the Fibre Content

The Arboform formula indicates a major dependence of the mechanical properties on the content of fibres (particularly hardwood fibres), which ensures a wide-range variation of the injection moulded parts material properties. Figure 11 indicates a significant increase of the tensile strength related to the fibres content within the composition using hardwood fibres. A 45% approximate content of fibres can provide a good balance between stiffness and strength. In the case of other fibre types (Figure 12), substantial high modulus is reached even though the fibre content might be lower [2, 14, 16].

The bending stress (Figure 13) registers an increase due to the content of fibers. Taking into consideration the same percentage, approximately 45%, the bending stress value is higher than the double value of tensile strength.

Concerning the indentation hardness (Figure 14) and impact strength (Figure 15) in relation to the fibre content, the dependence is less pronounced. The mechanical properties values are very close to those of wood-like plastics with commercial lignin.

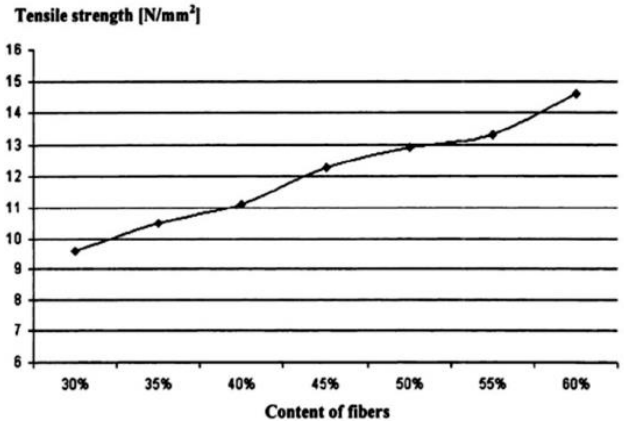

Fig. 11. Tensile strength vs. Fibre content [14, 16]

3.2 Microindentation

The Arboform microindentation results are listed in Table 4, according to the authors indicated in [17]. Figure 6 exhibits the microindentation variation values.

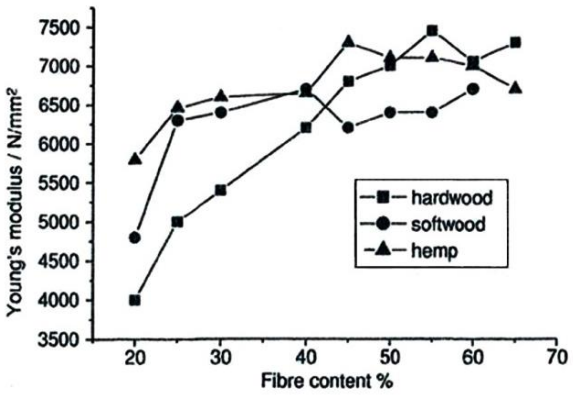

Fig. 12. Young's Modulus dependence on the fibre content [2, 14]

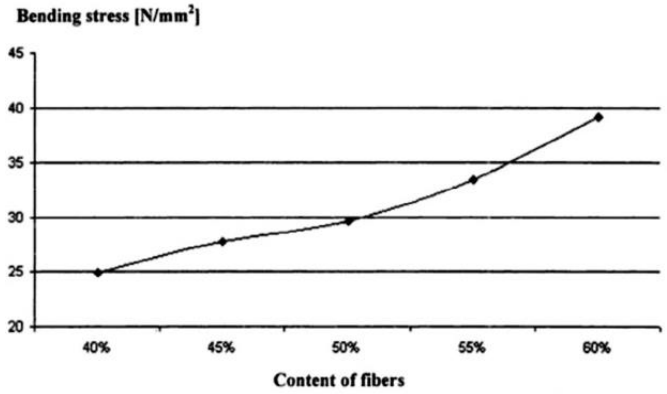

Fig. 13.Bending stress vs. content of fibers[14, 16]

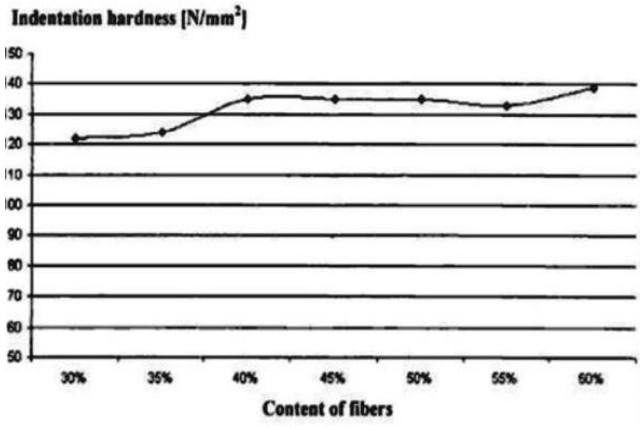

Fig. 14. Indentation hardness vs. fibre content [14, 16]

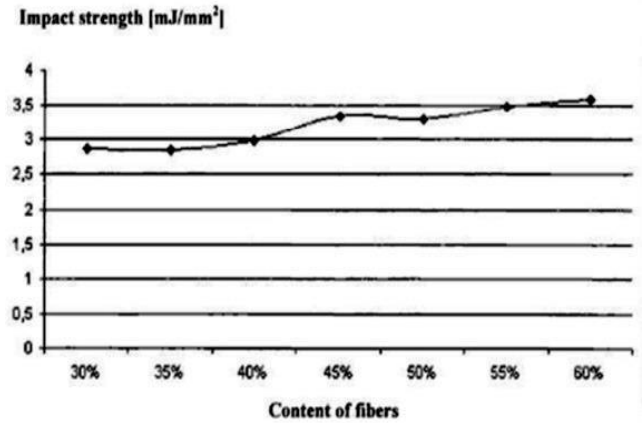

Fig. 15. Impact strength vs. fibre content [14, 16]

The microindentation tests were performed by means of a universal device UMT-2 (CETR-Center for Tribology Research, INC, USA). A 2kg sensor was also used by applying maximum load of 10N. Likewise, the testing performance implied use of a Rockwell diamond indenter having 200 µm radius. The capacity sensor implied in testing operations provided measurement of the vertical displacement of indenter.

The following Figure 16 presents the load diagrams elaborated based on the indenter vertical displacement. The applied soft has enabled reading of microhardness values, indentation modulus values, as well as the Young modulus data. These values are listed within Table 4 also indicating the displacement and recovery data for the three types of "liquid wood". The study was performed on three samples for each material. The relative density is calculated as ratio between the mass density and reference density (melt density at 170 °C). The output value is 1.06 [17].

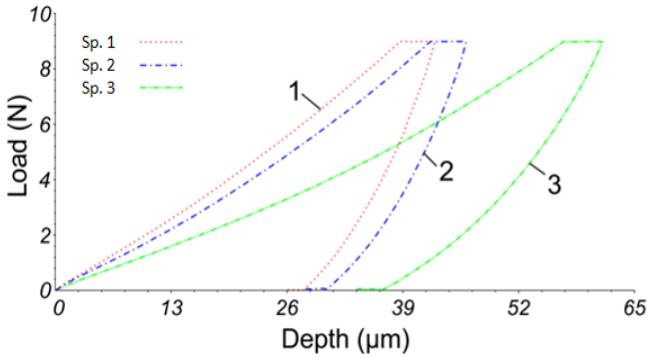

Fig. 16.Arboform L, V3 Nature Microindentation Test [17]

3.3 Impact strength

An improvement on compound processing would lead to an increase of impact strength well above 2 kJ/m^2. A further impact strength increasing requires incorporation of a significant amount of impact modifiers, which should be bio-compatible and biodegradable,at least [2]. Nevertheless, a broad range can now be covered as shown in Figure 17.

Tensile strength expresses how much a material can be stretched before breaking under high stress and at high speed. Fibers play a very important role in what concerns impact strength or material hardness.

The present study shows how the impact strength severely decreases on the incorporation of filling materials (Table 5).

Addition of 1% PMDI compatibilizer (polymeric methylene diphenyldiisocyanate) to lignin composites improves the impact resistance by 92% in comparison to that of non-compatibilizer correspondent. This improvement is possibly provided by plasticizing process. An increase of PMDI content, from 1% to 2%, caused small decrease in the impact strength of composites. The authors of the study referenced [32] have also reported the impact strength decrease to the PMDI increased concentration. The previously-mentioned authors

Table 4. Presentation of study results [17]

		Parameter					
Material		Material Displacement (µm)	Recovery (µm)	Micro Hardness (GPa)	Indentation Modulus (GPa)		Load (N)
					Reduced	Young's	
Arbofill Fitchie	Sp. 1	98.374	42.907	0.079393	0.805	0.826	8.941
	Sp. 2	94.205	35.604	0.0811	1.011	0.983	8.942
	Sp. 3	110.195	59.24	0.07364	0.591	0.575	8.934
Arboblend V2 Nature	Sp. 1	60.051	18.057	0.140298	2.617	2.547	8.965
	Sp. 2	63.996	21.793	0.128738	2.429	2.363	8.975
	Sp. 3	75.957	26.985	0.110428	1.419	1.38	8.954
Arboform L, V3 Nature	Sp. 1	42.575	12.673	0.231877	3.078	2.997	8.970
	Sp. 2	46.121	16.005	0.197364	3.541	3.449	8.978
	Sp. 3	61.361	24.551	0.150256	1.844	1.794	8.972

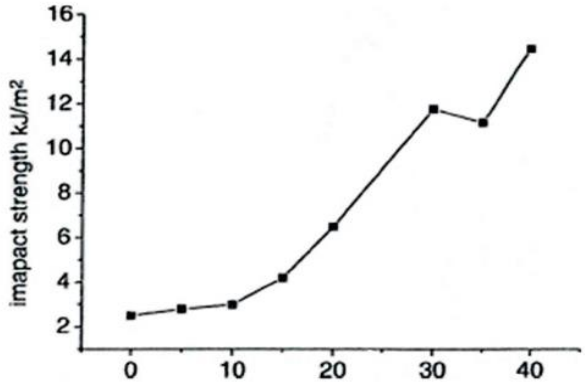

Fig. 17. Dependence of the impact strength on the amount of impact modifier used [2]

registered a negative effect at 1% PMDI during the use of bamboo cellulose composites. Moreover, the same effect was also observed at 2% content for the composites filled with lignin and presented in the study referenced in [28].

Similar tendency has been registered for the impact strength of notched Izod of the lignin composites - PP (polypropylene) [29]. It has been reported that incorporation of lignin, which is an unstable material, causes the composites impact strength to decrease. The incorporation of agrofibres also determines decrease of composites impact strength [30, 31].

Table 5. Tensile modulus, flexural strength, HDT (Heat Deflection Temperature) and impact properties of composites [28]

Specimen label	Tensile strength (MPa)	Tensile modulus (GPa)	Elongation at break (%)	Flexural strength (MPa)	Flexural modulus (GPa)	Impact strength (J/M)	HDT (°C)
PBS	35±1.5	0.6±0.01	122±21	28±0.4	0.6±0.01	40±8.4	78±1.9
30% Lignin-PBS	26±1.8	1.1±0.03	4.6±0.3	40±0.5	1.1±0.01	29±1.0	83±3.0
50% Lignin-PBS	29±3.4	2.3±0.35	2.0±0.8	46±0.3	2.2±0.03	15±0.9	86±3.1
65% Lignin-PBS	39±1.1	3.3±0.04	1.5±0.1	52±1.1	3.8±0.15	11±0.9	85±0.6
50% Lignin-PBS-1% PMDI	37±6.1	2.0±0.03	3.1±1.3	68±1.8	2.3±0.07	29±2.3	90±1.9
50% Lignin-PBS-2% PMDI	42±4.7	1.9±0.19	4.3±0.7	66±0.7	2.1±0.03	24±3.7	94±1.6

3.4 Tensile strength

Table 5 shows the composite tensile properties. It is noted that the composite tensile strength has initially reduced by 30% in the case of 30% incorporated lignin and then has gradually risen with the increase of lignin content to 65% (table 5). The composite tensile strength has also decreased with the increase of filler content (agro fibers) in the biodegradable polymers such as PLA (polylactic acid) and PBS (polybutylene succinate) [30, 31]. The result has been ascribed to poor interfaceadhesion between the hydrophilic filler and hydrophobic polymer matrix. However, the tensile properties of composites have improved in the case of higher lignin content (65%). Therefore, the tensile strength has risen by over 10% of 50% lignin-filled composites and the resistance was about 13% higher than the value of pure

polymer.
The increase of tensile strength in the case of higher lignin content points out the reinforcement effect of lignin in PBS polymer. This can be ascribed to the similarity in the solubility parameter of lignin and PBS, cross-linking capacity and lignin adhesive properties.
Viscosity in the composite melt has been noticed during processing the composites with 65% lignin filler. However, composite melt at 30% and 50% lignin content has been relatively less viscous. The above mentioned result may be ascribed to the lignin cross-linking capacity that grew with the increase of lignin content in the composite materials.
The composite elasticity modulus increases gradually with the rise of lignin content in the composite materials. The improvement of composite properties shows the possible polar-polar interaction between lignin and polyester matrix. The improvement of tensile strength of hydroxypropyl lignin and polyethylene mixture with an addition of vinyl acetate, polar component in the polyolefin non-polar matrix, also stands for the interaction concept [33]. The authors have interpreted the interaction due to the presence of polar carbonyl group [33]. Therefore, formation of hydrogen bonds might be possible between the carbonyl group of polyester matrix and the hydroxyl group of lignin.
Based on adequate processing and combination of properties, 50% filler-based composites have been selected for PMDI compatibilizer incorporation. The incorporation of 1% and 2% PMDI has increased tensile strength by 27% and 44% in the non-compatibilized composites and has been almost 7.5% and 22% greater than the value of the pure/clean polymer (table 5). These results back up the conclusion that PMDI enhanced interface adhesion in composites [32, 34].
PMDI addition leads to the formation of (-HN-COO-) urethane, bond created due to the reaction between –NCO group ofPMDI and –OH group of lignin [35]. Furthermore, the urethane bond may lead to the secondary intermolecular join (e.g. hydrogen bonds between N-H group of urethane bond and carbonyl bond of polyester, [35]) that might be the reason for the enhancement of interface adhesion of PMDI compatibilizer composites.
The composite modulus slightly decreases with 1% PMDI addition (table 5). The composite modulus has been gradually reduced with rise of PMDI concentration from 1% to 2%. The modulus decrease may be ascribed to the plasticization of composite materials due to PMDI addition. The humidity in bio-filler has been reported to respond to PMDI and to produce amine or urea compounds.
The above mentioned compounds plasticize the composites [34], resulting in modulus decrease and elongation increase. The stress – strain curves of composites are presented in figure 18.
The figure also depicts the fragile behavior of composites. The materials tensile stress decreases with the incorporation of filler and is slightly improved by PMDI addition. Table 5 shows how breaking elongation value reduces with filler incorporation, and slightly increases with PMDI addition. PBS is extremely ductile polymer; the elongation percentage reduces significantly by 10% the moment the bio-filler is added [36]. Similar trends of properties upon PMDI addition are to be observed for sugar beet pulp in the polyactide-based composite [34].
The mixture rule is contained in equation (1) used to determine the composite modulus, and is usually applied to randomly oriented short-fiber composites. [30].

$$E_c = V_m E_m + kV_f E_f \quad (1)$$

where: E_c, E_m, $E_f$represent elasticity moduli of composite, polymer matrix and filler material (lignin), respectively. The lignin modulus 6.27 GPa [6] has been considered to calculate the composite modulus; $V_m$andV_f represent the volume fraction of polymer matrix and filler material, respectively. Factor "k" (contribution of fiber length and orientation) has been used to match the data.The fraction related to fiber and matrix volume has been calculated using PBS (1.26 g/cm^3) and lignin (1.34 g/cm^3) density.
Table 5 shows the correlation between the theoretical modulus and the composite modulus determined experimentally. The increase of modulus with the growth of lignin content is evident in figure 19.
The theoretical modulus calculated by mixture rule has been greater than the composite modulus experimentally determined. Considering the matching parameter k = 0.67, the theoretical modulus matches exactly with the experimental modulus of the 50% lignin filled composite. However, the modulus values obtained in the case of composites with 30% and 65% lignin filler have been slightly lower and greater than the values of the calculated modulus.
Considering the random orientation of wheat straw fibers, the authors have reported a fiber efficiency coefficient of k = 0.9 [31]. However, lignin grains (with fine milled 45% bio-fibers, lignin particles and other additives [6.38]) have been used as filler material instead of bio-fibers. Therefore, the value of the coefficient "k" = 0.67 is reasonable enough. The interaction polymer – lignin (that is not considered in the equation) may result in low values of the modulus for composite with 30% lignin content, high values of the composite with 65% lignin content and modulus theoretical values.

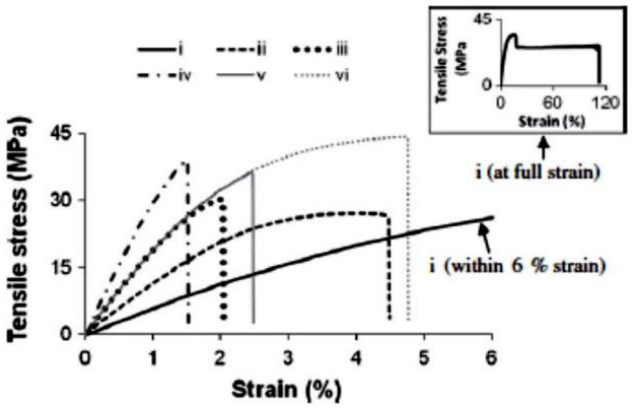

Fig. 18. Stress – strain curve of composites: (i) PBS pure specimen, (ii) 30% lignin PBS composite, (iii) 50% lignin PBS composite, (iv) 65% ligninPBS composite, (v) 50% ligninPBS composite with 1% PMDI , (vi) 50% ligninPBS composite with 2% PMDI, [28]

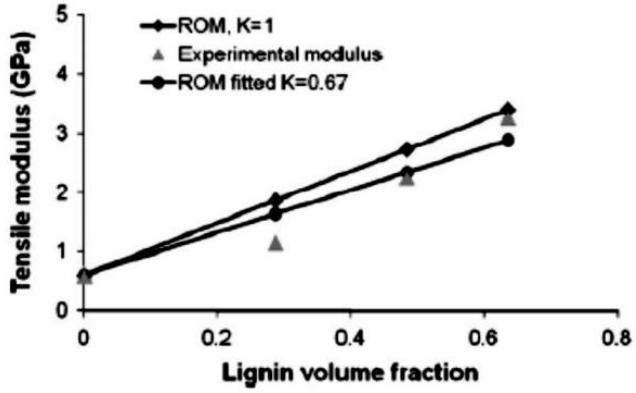

Fig. 19. Correlation analysis: experimental elasticity modulus and mixture rule (ROM), [28]

3.5 Mechanical properties: bending

As can be seen from table 5, the bending strength and the coefficient of elasticity of composites has gradually increased with the lignin content. The bending strength and the coefficient of elasticity rose from 41% to 84% and from 81% to 503%, respectively with the increase of the lignin content 30-65 %. The polar bio-filler are considered to be compatible with the polar polymers that enhance the two phase blending possibility and promote a better interfacial morphology [28].

However, the difference between the bending strength and the coefficient of elasticity variation has not been clearly understood. The mechanical behavior of the material under tension and bending stress may be the cause of the variation. The addition of 1% PMDI improves the bending strength by 48% as compared to the non-compatibilized material, and by 143% as compared to the pure polymer (table 5). The stress transfer from the matrix to the filler and towards a compatibilizer-modified interface is considered to be the cause of the significant improvement. The coefficient of elasticity of the composites with 1% compatibilizer agent remained to almost the same level of the coefficient of the non-compatibilized materials (table 5). The increase of PMDI to 2% has slightly decreased the bending strength and the coefficient of the composites. This result may be ascribed to the effect resulted from different concurrent reactions, such as the formation of urethane bond and secondary hydrogen bonds [28].

3.6 Dynamic mechanical analysis (DMA and HDT analysis)

The dynamic mechanical analysis (DMA) is widely used to investigate the structure, elasticity and viscosity of the composite materials. The delay measurement ($T_{an\delta}$) provides information on glass vitreous transition temperature, and the build-up modulus provides data on stiffness. The build-up modulus records the elasticity component of the material complex modulus. Figure 20a shows the storage and loss moduli and $t_{an\delta}$ of the composites according to temperature. The polymer and composites storage modulus decreased with the increase of temperature (figure 20a). The reduction of the storage modulus with the temperature may be ascribed to polymer softening and to the fact that the mobility of the polymer matrix chain increases at higher temperatures. As compared to pure PBS, the composite storage modulus at room temperature (25 °C) grew by 96-495% to 30-65% at the same time with the increase of lignin content. Similar results have been noticed in the case of agro-flour contained by the biodegradable composites [30]. The composite storage modulus remained almost constant to 1% PMDI addition. However, the storage modulus increases and decreases with the 2% PMDI content. This remark may be ascribed to different concurrent reactions caused by PMDI addition.

The decrease of the storage modulus represents the contribution of the viscosity to the material complex modulus. At room temperature the loss modulus of certain composites has increased with the growth of filler content (figure 20b). However, a very small difference has been identified in the loss modulus near the glass vitreous transition temperature [37]. The glass vitreous transition temperature (T_g) given by the peak of the loss modulus (figure 20b) grew with the increase of the lignin content. Two peaks may be noticed in the thermogram of the composite with 65% lignin: the first peak corresponds to the Tg polymeric phase and the second represents the filler (due to the high filler content). The compatibilized addition to the PBS composite with 50% lignin filler has slightly decreased because of the glass vitreous transition temperature.

The material delay behavior is measured by $T_{an\delta}$ magnitude, which represents the relationship between the loss modulus and storage modulus or between the dissipated and stored energy during the adynamic loading cycle [38].$T_{an\delta}$ decreased with the filler incorporation (figure 20c). The result shows that the addition of filler decreased the molecular mobility of the composite materials and that the mechanical

losses contribute to passing over the inter-friction between the molecular chains that are also reduced. A similar remark has been reported with regard to reinforcement of the composites with PBS [38] and PLA [30] bio-fibers.

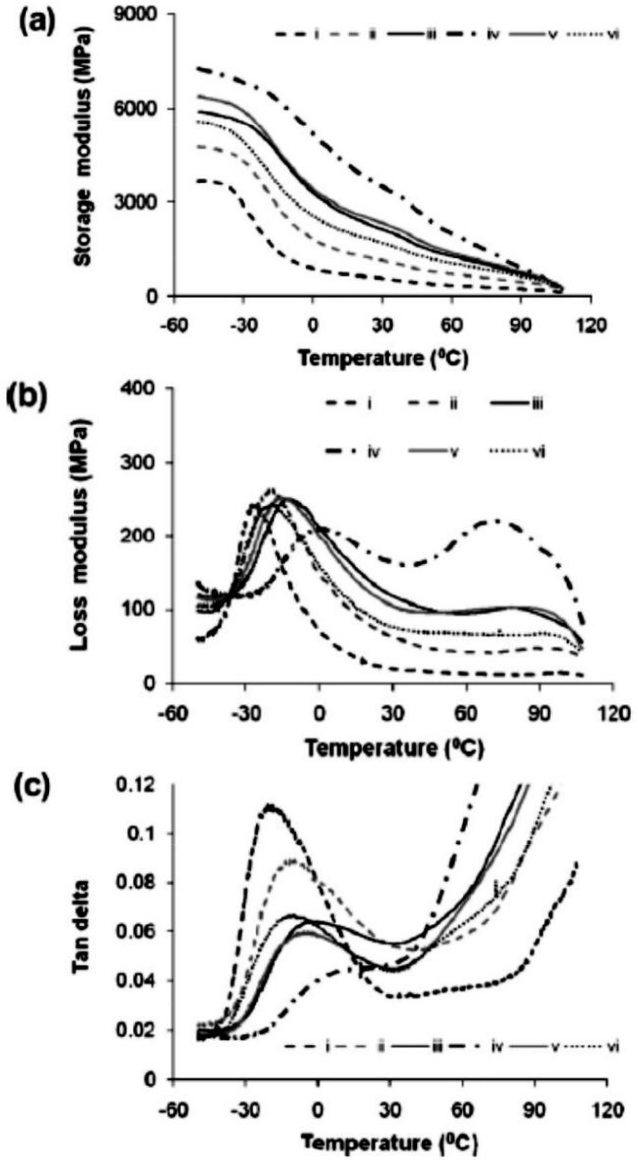

Fig. 20. Dynamic mechanical analysis: (a) storage modulus, (b) loss modulus (c) $T_{an\delta}$of composites. (i) PBS pure sample, (ii) 30% lignin- PBScomposite, (iii) 50% lignin- PBS composite, (iv) 65% lignin-PBScomposite, (v) 50% lignin-PBS composite with 1% PMDI , (vi) 50% lignin-PBS composite with 2% PMDI, [28]

The interaction between PBS matrix and lignin can be understood by the increase of the temperature of $T_{an\delta}$peak (often mentioned as vitreous transition temperature, T_g) and enlargement of thermograms$T_{an\delta}$ as a result of lignin incorporation. Two effects are considered to determine the cause of T_g increase. The first effect may be the creation of an amorphous component in the composite structure in which both polymer and filler coexist in a closely associated condition and contribute to the reduction of free volume in the composites. As a result T_g increases. T_g may also increase due to secondary bonds that act as quasi-crossed (reticular) bonds and limit the Brownian motion of long chains [33]. Firstly, composite T_g has increased to 1% and then decreased by almost 6°C when 2% PMDI has been added. This fact may be ascribed to such effects as improvement of interaction and plasticity due to PMDI added. The interaction between polymer and filler improves T_g, and plasticity decreases T_g in a material.

Heat deflection temperature (HDT) is a measure of the material dimensional stability under a certain load and temperature. This is considered essential requirement of the property for a wide range of material applications. Table 5 shows HDT values for pure PBS and all composites. HDT of composites grows with the increase of lignin content to up to 50% of weight and stays almost unmodified with the increase of lignin up to 65%. The improvement of HDT has also been noticed in the composites with bio-fiber reinforcement [39, 40], which may be ascribed to high crystallization of bio-composites [39] in comparison with pure composites. The incorporation of compatibilizer improves HDT of composites as a result of interfacial adhesion enhancement [39].

4. ELECTRICAL PROPERTIES

4.1. Electrical conductivity with nanoparticles

There are various approaches to increase electrical conductivity of plastics by means of nanoparticles [41, 42]. Precipitation of metallic nanoparticles in the case of reinforced fibers is an efficient approach to achieve good electrical conductivity at low concentrations. To avoid oxidation during extrusion and mould injection processing, Pt has been selected as metallic particles model. Pt stable suspensions (delivered by Tsutomu Sakai, KR1 Inc, Japan) [43] have been applied in two variants of concentration: suspension 1 (150 mg Pt/ L) and suspension 2 (1500 mg Pt/ L). Both variants contain 2-5 nm sized particles (figure 21). The fibers have been immersed in suspensions and precipitated particles in a rotary evaporator with vacuum system to remove liquid medium at 70 °C. Different types of fibers have been investigated, including glass fibers, PA (polyamide), PET (polyethylene terephthalate) and natural hemp and wood fibers, by means of composites with lignin matrices [44].

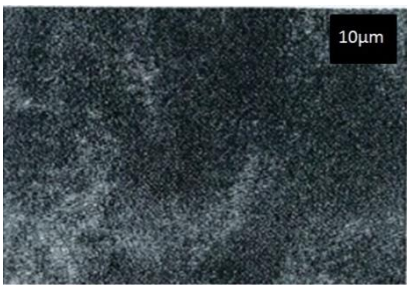

a)

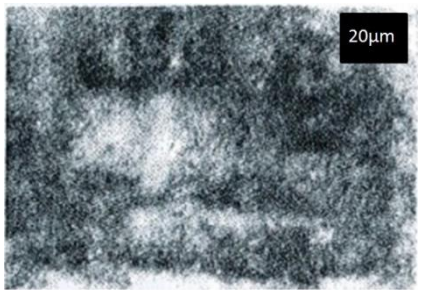

b)

Fig. 21. Deposit of Pt on natural fibers; left image (a): with suspension 1 (150 mg Pt/ l) orsoftwood fibers; right image (b): suspension 2: (1500 mg Pt/ l) on hemp fibers [2]

4.2. Electron energy loss spectrometry (EELS)

EELS measurements (figure 22) indicate a change in the hybridization of a structure rich in sp^2 following pyrolysis. This can be read from the presence of plasmon-π at 6 eV electron energy loss [45]. Unpyrolyzed free fibers generate severe loads during measurements, and intensity drops suddenly with every scan.

Therefore, figure 22a shows only the first several scans, the average and the explanations of the noise weak signal in relation to the measurements performed on materials containing carbon fibers. The signal of the carbon fiber containing compounds has been stable throughout the measurement period. Following pyrolysis at 1200°C, plasmon-π rises and a sharp structure is generated, which indicates the conversion to a similar graphitic material. Furthermore, plasmon-π is found at an energy loss of almost 25 eV, usually measured for graphite [46]. This fact supports the existence of a graphitic structure.

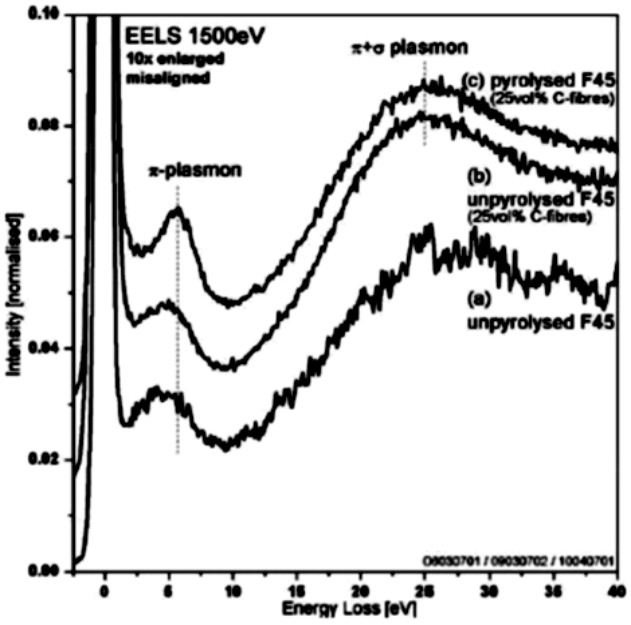

Fig. 22. EELSspecter of unpyrolyzedArboformwithout (a) and with carbon fibers (b) as compared with pyrolyzedArboform with carbon fibers (c), [44]

4.3. Electrical conductivity

Electrical conductivity has been determined by means of various Arboform F45 samples that have been submitted to pyrolysis at different temperatures. For purposes of comparison, the conductivity of Arboform with 25% carbon fibers, submitted to pyrolysis up to 1200 °C, has also been tested. The electrical conductivity values did not fluctuated significantly during different sample measurement points; thus conductivity is isotropic. Table 6 summarizes the average values of the electrical conductivity.

Table 6. Electrical conductivity ofpyrolyzedArboform F45 sample measured by four-probe method [44]

Sample	Pyrolysis	Electrical conductivity (S cm^{-1})
F45	600 °C	0.49
F45	1000 °C	7.5
F45	1200 °C	0.0053
F45 with 25% C-fibers	1200 °C	164 (along fiber direction)
F45 with 25% C-fibers	1200 °C	44.6 (cross fiber direction)

Electrical conductivity varies with pyrolysis temperature. Furthermore, the presence of carbon fibers is important. UnpyrolyzedArboform F45 is a polymer, an insulating material that cannot be characterized by means of four-probe method. Arboform F45 pyrolyzed at 600 °C is a weak conductor. The sample/ specimen pyrolyzed at 1000 °C, with 7.5S cm^{-1} conductivity, are an example of reasonable conductivity. The use of carbon fibers increases drastically the conductivity. The measured conductivity was much greater along than across fiber direction. The value of electrical conductivity of the sample without carbon fibers, pyrolyzed at 1200 °C is very low. This low value is ascribed to the fact that pyrolysis at high temperature results in porous material due to pyrolysis gas diffusion. The holes created by gas diffusion might disappear in future in the case of pyrolysis process optimization.

5. THERMAL PROPERTIES

5.1. Fire resistance

The realization of certain fire retardant class is difficult to achieve when only bio-base or at least bio-compatible substances are used. To obtain relevant values, the additive quantities required are high and may negatively influence frequently the mechanical properties. Only halogen free additives, which impact on environment is justified, are used. In the case of synthetic plastics, such as large polypropylene quantities, these types of additives must be used to

fulfill some basic criteria. Arboform composite with lignin matrix requires smaller quantities of fire retardant substance to achieve fire/ fire-set rating: UL V1 (Underwriters Laboratories –combustion stop within 30 seconds for vertical specimen) and UL HB(Underwriters Laboratories – slow combustion for horizontal specimen). The mechanical properties are simply reduced by 10-20%.
UL V0 (Underwriters Laboratories –combustion stop within 10 seconds for vertical specimen) and UL HB rating are also possible, [2].

5.2. Pyrolysis of porous carbonic structures

Arboform submitted to pyrolysis leads to porous carbonic structures that can be used for various applications [47]. The injected parts submitted to pyrolysis might allow the realization of complex forms created in mould. The result is a graphical structure (figure 23) with high porosity (figure 24). Moreover, the high degree of porosity might allow the pyrolyzedArboform to act as isolating material or wear resistant material and to remain thermally stable at high temperatures.

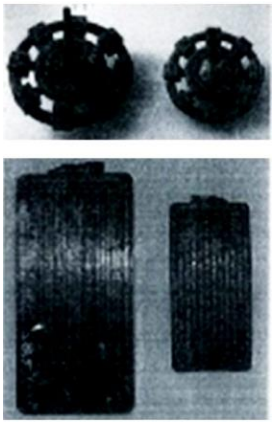

Fig. 23.Pyrolysis of Arboformleads to a stable component that can be used for various carbon applications [2]

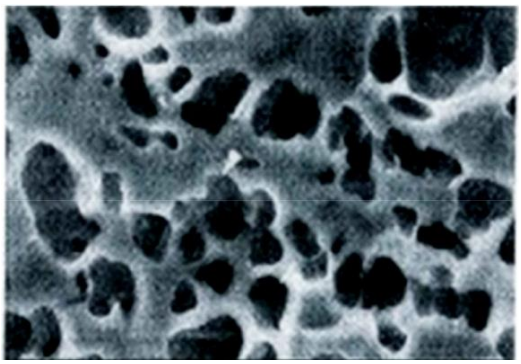

Fig. 24.Porous structure of pyrolyzedArboform [2]

Ceramics (e.g. metallic carbide) can be obtained in the case of metallic-organic compounds infiltration to produce a metal or a metal oxide layer in decomposition. A new possibility might be deposit of Si (silicon) in cyclopentasiloxane in accordance with the description of glass fibers [48, 49]. The electrical conductivity of carbonic material varies with pyrolysis temperature and may be modified by additives.
The presence of carbon fibers in Arboform may also stabilize the structure acting as precursor. UnpyrolyzedArboform F45 is a biocomposite with low electrical conductivity; this means that the unpyrolyzedArboform F45 is an isolating material. The material conductivity may be controlled on one hand by precipitation of metallic particles on reinforced natural fibers, and on the other hand by modification of pyrolysis temperature. When the conductivity of pyrolysis at 600°C is still low as a result of pyrolysis at 1000 °C, a reasonable value of conductivity is obtained. This value decreases substantially when the material is pyrolyzed at 1200 °C, [44].

5.3. Pyrolysis of wood-based polymeric compounds

To improve thermal and mechanical stability and increase conductivity the carbon fibers may be added to the base material. Pyrolysis has been carried out at 1200 °C under nitrogen atmosphere, which leads to continuous increase of conductivity. Following pyrolysis the samples have been investigated by means of surface scientific techniques [50]. Arboform F45 has been used in the procedure. The carbon fibers have been mixed previous to injection process to improve thermal stability and increase conductivity. The carbon fibers Tenax-J HT C261 3 mm andTenax-J HT C604 6 mm are almost 3 mm in length and are based on polyacrylonitrile [51]. Due to this fact, the carbon fibers contain nitrogen [52] that is based on polyacrylonitrile. To increase humidity and reactivity, the polyacrylonitrile is oftenoxidized by means of resin matrix [51]. Arboform matrix contains 25% carbon fibers and ensures optimal enhancement of the material properties maintaining the wood the main component. Pyrolysis under nitrogen atmosphere has been carried out subsequently at 1200°C to graphitize the specimens. Following pyrolysis up to 1200°C the shrinkage of all specimens is almost 30% in each direction.
The samples have been later transferred to ultra high vacuum (base pressure $p \approx 10^{-10}$ mbar) to be submitted to X-ray photoelectron spectroscopic analysis (XPS), electron energy loss spectrometric (EELS) analysis, and to advanced vacuum ($p \approx 10^{-7}$ mbar) to run scanning electron microscopy (SEM). XPS measurements have been carried out using non-monochromatic MgKα (1253.6 eV), X-ray source (Leybold, V= 12 kV, I=20 mA). Two up to four scans have been recorded with binding energy of 50 eV.
Fine scan for compounds containing carbon fibers has been measured using binding energy/ pitch of 10 eV. The binding energy has been calibrated on a peak of Au 4f la 84.0 eV, with integral width measured at

maximum half of almost 1 eV, [53].
The pitch width has been established at 0.1 eV for each case. EELS measurements have been carried out using an electron beam with 1500 eV energy. The current beam adjusted according to similar intensities of the elastic peak (electron gun of Leybold-Heraeus) has also varied. Throughout the measurements, 10 scans with energy pitch of 10 eV have been carried out. All XPS and EELS measurements have been considered in normal emission. Emitted electrons have been analyzed by ahemisphericalanalyzer (Leybold-Heraeus EA-10).
Scanning electron microscopy (SEM) measurements have been carried out under vacuum conditions, beam energy 20 keV and 4-8 mm distance (Zeiss/ LEO Supra 55 VP).
The specimen electrical conductivity has been measured at surface by the four-probe method. Upon configuration, current can be adjusted from 0 to 200 mA and voltage from 0 to 2 V. All measurements have been carried out at room temperature.

5.4. Differential scanning calorimetry

The effect of lignin on the crystallization and melting behavior of composites has been studied during non-isothermal DSC experiments. The crystallinity degree has been determined based on the following equation, (2), [30, 40]:

$$\chi(\%) = \frac{\Delta H_m}{f \cdot \Delta H_m^0} \times 100 \quad (2)$$

where: χ = crystallinity degree (%); ΔH_m = enthalpy of melting of the material under study; ΔH^0_m = enthalpyof meltingfor PBS 100% crystalline, i.e. 210 J/g, [34]; f = weight fraction of polymer in composite. The glass transition temperature (T_g) rose from 5-19 °C at the same time with the increase of lignin content in the composite (Table 7), which indicates the adequate interaction between the polymer matrix and lignin. The lignin acts like a PHB composite forming agent and eases crystallization, [54]. The crystallinity degree rises when up to 50% of the filler is incorporated and slightly falls when the filler content reaches 65% (Table 7). The value of the lignin content (amorphous in nature) might have had a role in the crystallization of polymer germs.
The decrease of the crystallinity of the polymer with 65% lignin may be compared to the polymer matrix due to the high content of filler. The lignin has no effect on the melting behavior of the polymer.
However the addition of PMDI compatibilizer results in the decrease in the composite crystallinity; if the PMDI content varies, the effect is inconsistent. Similarly, once the PMDI content increases, the vitreous transition temperature has different trends. Although the PMDI effect on the heat properties of the composites based on natural filler is not clear enough [34], the interaction of the polymer filler andplasticization due to PMDI addition may be considered as cause of the results.
DSC has been carried out on pieces of Arboform L, V3 Nature of maximum 25 mg; three specimens have been tested. The experiments have been carried out on a differential scanning calorimeter (DSC) of F3 Maia type delivered byNETZSCH Company in argon shielding gas environment.
DSC F3 Maia calorimeter has the following characteristics: temperature range (-170 ... +600)°C; heating rate (0.001 ... 100) K /min; cooling speed (0.001 ... 100) K /min; temperature measurement precision 0.1 K; sensitivity <1 μW; enthalpy measurement precision ± 0.5%. The apparatus has been calibrated on Bi, In, Snand Zn, according to standards. The specimens have been warmed at room temperature at 423 K, heating speed $1.67x10^{-1}$ K s^{-1}, and then cooled at room temperature.
Proteus software has been used to assess the DSC thermograms recorded during the heating process. The critical transition points: initial transition temperature (T_s), middle transition temperature (T_{50}) and final transition temperature (T_f) have been calculated by tangent linear method. The dissipated and absorbed heat (DH) has been determined by means of a sigmoid reference line, [17].
Figure 25 shows the calorimetric reaction (DSC-thermal flux variation) of the pieces taken from three testing samples that have been submitted to heating up to a temperature of 423 K under control.

Table 7. Heat properties of DSC-obtained composites, [28]

Types of specimen	T_g(°C)	T_m(°C)	$\Delta H_m\ (J/g)$	T_c(°C)	$\Delta H_c\ (J/g)$	χ (%)
PBS	-31.1	113.2	64.8	78.4	62.2	30.9
30% Lignin-PBS	-26.4	112.0	57.3	71.6	43.7	39.0
50% Lignin-PBS	-20.5	112.0	49.1	64.3	31.6	46.8
65% Lignin-PBS	-12.1	110.4	31.6	63.9	21.6	42.9
50% Lignin-PBS-1% PMDI	-15.8	111.6	25.7	77.2	25.5	24.7
50% Lignin-PBS-2% PMDI	-21.1	110.9	26.3	76.9	27.03	25.6

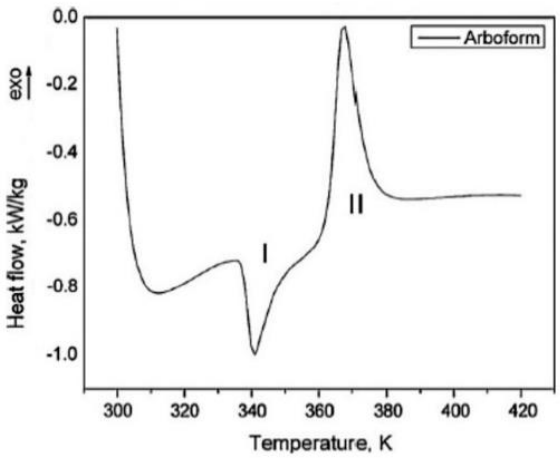

Fig. 25. DSC thermogram recorded during Arboform L, V3 Nature specimen heating, [17]

As can be seen from the graph two peaks are shown on DSC thermograms: (i) an endothermic peak occurs during heating from room temperature up to 350 K (I) and (ii) an exothermic peak of higher intensity occurs during heating at temperatures greater than 350 K (II). The endothermic peak takes place within the temperature range (337-347) K as per the data delivered by Proteus software for the tested Arboform specimens. The greatest difference of 1.7 K has been recorded for the temperature related to completing the transition T_f.

The deviation of heat flux from linearity suggests the presence of a solid endothermic state; the transition takes place when both testing specimens are heated.

The second transition to solid state (II) is exothermic; besides the initial transition temperature - T_s II, the other critical transition points occur at about same temperatures. The variation of the thermal flux can be assigned to a solid state transition which occurs at heat generation.

Table 8 summarizes the data evolution by means of Proteus software and tangent method used to determine critical temperatures (Ts, T50 andTf) and sigmoid reference value to obtain the absorbed/ dissipated specific heat Δh, [17].

The analysis of the absorbed and dissipated heat during the two transitions to the solid state, which have been recorded regarding the specimenArboform L, V3 Nature (heated up to a temperature of 423 K), points to the following trends:

• By comparing the heat absorbed by the two specimens during the first endothermic transition and recorded throughout the heating process, it is evident that, to allow transition, specimen Arboform L, V3 Nature requires twice the heat needed for the specimen Arboblend V2 Nature.

• By comparing the heat absorbed and dissipated by the same heated material, it is evident that the exothermic transition of specimen Arboblend V2 Nature is greater Δh I = -5.654 while Δh I = 19.38 kJ / kg. This ascending trend is recognizable for specimen Arboform L, V3 Nature, [17].

5.5. Thermogravimetric analysis

Table 9 shows the initial thermal degradation, weight loss (%), maximum degradation temperature and charred residues remained after applying temperatures of 600°C in the case of lignin, pure polymer and composites. The initial degradation of lignin and PBS polymer is carried out at 179°C and 306.4 °C, respectively. The initial degradation and maximum degradation of composite materials has decreased once the lignin content rose. The composites with 50 and 65% lignin content exhibited very close initial degradation temperatures. The addition of PMDI in lignin-PBS composites raises the initial degradation of composites by 7°C.

Weight loss at about 100°C may be caused by loss of humidity in materials, and initial thermal degradation may correspond to cleavage of weak ether bonds [35] present in lignin interunits (bond β-O-4). The maximum degradation temperature of lignin was much smaller than the maximum degradation temperature of pure polymer.

In contrast to polymer, the peaks/ additional peaks have occurred on the curves derived from lignin. Two maximum decomposition peaks at temperatures between 340-345°C have appeared in the composites with high lignin content (50% and 65% of weight).

As has been previously discussed, the decomposition of lignin takes place as a result of more concurrent reactions that release more gaseous components.

In comparison with pure polymer and composites, a small weight loss percent has been noticed as regards lignin at a temperature of 400°. The greatest amount of residue (31.6%) following charring at 600°C was obtained in the case of lignin due to the high ratio of very condensed aromatic compounds.

Table 8. Summary of data evolution, [17]

Sample	**$T_{s\,I}$ (K)**	**$T_{50\,I}$ (K)**	**$T_{f\,I}$ (K)**	**Δh I (kJ/kg)**	**$T_{s\,II}$ (K)**	**$T_{50\,II}$ (K)**	**$T_{f\,II}$ (K)**	**Δh II (kJ/kg)**
Arbofill Fitchie	-	-	-	-	-	-	-	-
Arboblend V2 Nature	337.4	341.2	345.4	-5.654	359.6	366.3	374.5	19.38
Arboform L, V3 Nature	337.6	341.0	347.1	-11.94	363.1	367.6	374.2	28.08

The charred residues rose at the same time with the increase of lignin content in composites. The addition of PMDI compatibilizer has slightly raised the percent of charred residues in composites, which may be related to the presence of aromatic components of PMDI. The output is directly related to the material fireproof potential, [36]. Therefore the lignin fireproof capacity is expressed by this result, which relates to PMDI addition.

The optical microscopy shows that a larger quantity of hardwood (figure 27) is integrated in the lignin matrix. On the other hand the softwood fibers (figure 28) require more lignin to be entirely covered. As a result, good mechanical properties are already obtained at smaller fiber content and cannot be enhanced at fiber content greater than 45-50%.

Fig. 27.Microscopic shots of hardwood fiber present in different quantities, [2]

Table 9. Thermogravimetricanalysis of composites, [28]

Specimens	Degradation onset (°C)	Weight loss at degradation onset (%)	Maximum degradation temperature (°C)		Weight loss at 400°C (%)	Charred residues at 600°C (%)
PBS	306.4	1.0	402.9	-	57.1	0.2
30% Lignin-PBS	260.3	2.4	392.3	-	67.8	12.0
50% Lignin-PBS	237.6	2.6	387.9	343.2	63.8	20.4
65% Lignin-PBS	236	2.7	383.7	341.3	57.5	27.3
50% Lignin-PBS-1% PMDI	244.5	2.4	388.1	344.2[h]	61.7	22.1
50% Lignin-PBS-2% PMDI	236.7	2.6	357.8	353.1	62.6	21.8
Lignin	179	3.2	341	380-480[b]	53.4	31.6

[b]Broad; [h]Hump

6. STRUCTURAL ANALYSIS

6.1. Analysis of material breaking area

Processing results in an efficient bond achieved between fibers and lignin matrix, characterized by uniform fiber distribution, binder free. It is clear that at the breaking areas of material submitted to linear stress, fibers are not pulled out of the matrix, which confirms good bonding behavior (figure 26).

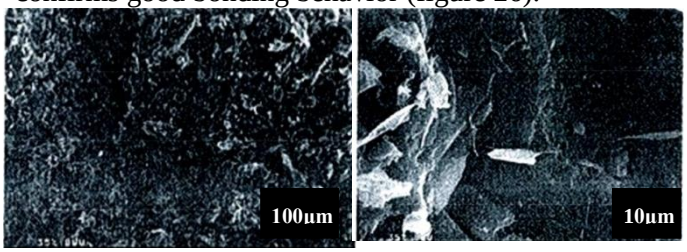

Fig. 26. Breaking area of tensile-stressed specimens, broken fiber and matrix are noticeable, [2]

Fig. 28.Microscopic shots of softwood fiber present in different quantities, [2]

Different types of fibers have been investigated, including glass, PA, PET, natural hemp and wood fibers used in composites with lignin matrix. The fibers have been incorporated in material to obtain composites by typical processing methods. SEM and RDAX have been applied to analyze deposited Pt. The fibers have been pressed as strands/ bands to measure electric resistance of specimens with 5-mm thickness and electric contacts found at 12 mm distance. Uniform layers are formed on fibers with Pt concentrations between 0.01 and 1%. The configuration of fiber surface determines the thickness of metallic layers and concentration.

The electric resistance of the pressed fiber band varies with the pressing conditions and may decrease from 10MΩ to 0.1 MΩ. Larger quantities of Pt are deposited on natural hemp fibers with rough surface structure (figure 29). A composite with bio-polymeric lignin matrix has been processed for standard tests. The electric resistance of this material has been reduced essentially in the described configuration from almost 10^4 MΩ to 10^1MΩ. These values are of interest for the surfaces used in electronic circuits. The risk of deterioration of semiconductor components does not exist.

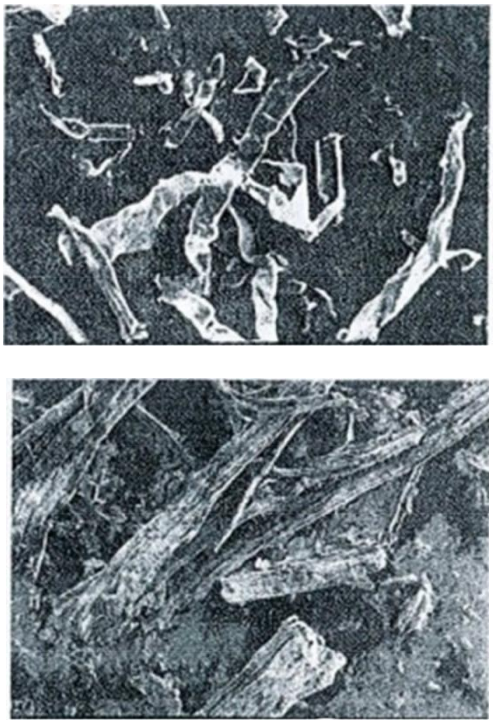

Fig. 29. Pt deposit on natural fibers, with Pt-suspension 2 (1500 mg Pt/ l): left image (a): on softwood fibers; right image (b): on hemp fibers, [2].

6.2. Scanning electron microscopy (SEM)

The structure and morphology of specimens have been examined by SEM. Both surface and cross section have been measured, as evident in figure 30. The fibers align in flowing directions due to injections in matrix.

The orientation of carbon fibers is incorporated in Arboform material (figure 30). The carbon fibers are likely to form the spine and the Arboform is the filler which bonds the whole material they make. This might be the explanation for the enhanced shape and stability of the rich form following pyrolysis.

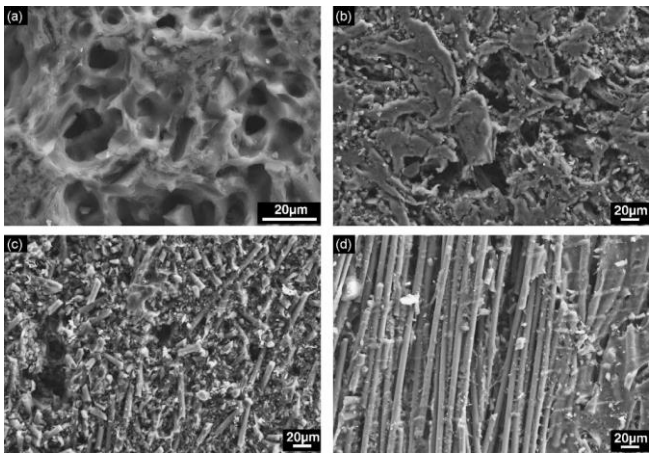

Fig. 30. SEM shots of Arboform (a and b) and C fibers containingArboform (c and d) normal at surface (a and c) and cross section (b and d). The orientation of C fibers is evident and results in dependent directional conductivity, [44]

6.3. Surface morphology

Figure 31 shows SEM images of composites. The separation of phases between polymer and filler is clearly noticeable in the rich side of the polymer with 50%-lignin content filler the PBS composite (figure 31a). The small quantities of reticular components existent in the filler of the composite material determined the occurrence of the above-mentioned fact. However, a more uniform distribution of the polymer and lignin filler may be noticed in the microphoto of the composite with 65% lignin filler (figure 31b). The data on tensile strength concerning these composites (with 50 and 65% lignin filler) also support this observation.

The micrographs at highermagnified (figure 31c and d) accurately describe the precise fraction of the surface morphology of the two composites. More pulled-out fibersand holes in the composite filled with 50% lignin indicated poor interfacial adherence. The possible cause of the higher number of out pulled fibers in the composite with 50% lignin filler may be the phase separation. In contrast, the number of interactions was greater in the composite with 65% lignin mainly because of the higher lignin content. The fiber obtained by means of resin matrix and a more compatibilizer phase indicates strong interface in the composites with 1% PMDI (Figure 31e). The enhanced interface reflects in the mechanical properties of the compatibilized composites.

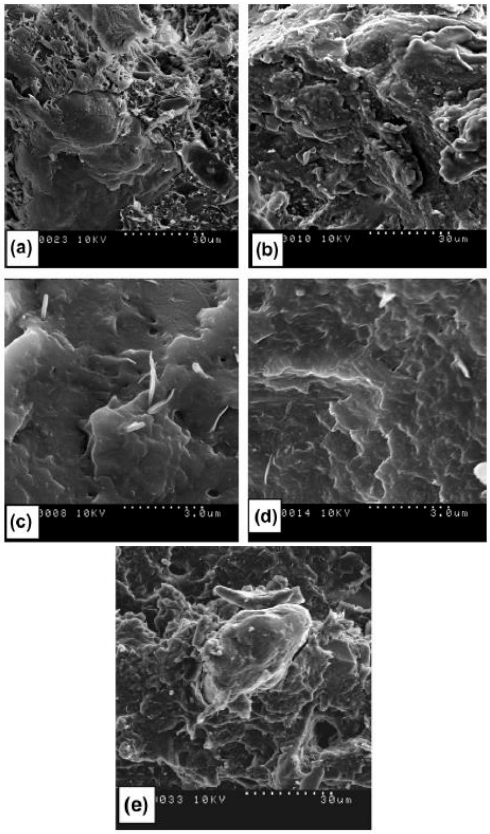

Fig. 31.SEM micrograph of composites (a and c) 50% lignin-PBS composite (lower and upper magnification rate, respectively), (b and d) 65% Lignin-PBS composite (lower and upper magnification rate, respectively), (e) 50% lignin-PBS with 1 % PMDI (lower magnification), [28]

7. X-RAY PHOTOELECTRON SPECTROSCOPY *(XPS)*

Figure 32 offers a general overview of the specter to notice all components and contamination degree. Based on the maximum surfaces of the elements detected and corresponding fine scanning, the atomic concentration of the elements detected has been calculated. For the purpose of this analysis, the cross sections and asymmetry parameters were taken from Yehand Lindau, [55]. The analyzer transmission was considered proportional to 1/ E_{kin}, which is typical for the hemispherical analyzer employed. Table 10 shows the compositions obtained for the samples analyzed.

However following pyrolysis, almost 70% of mass is desorbed as a result of NA enrichment, which may be detected by XPS. The real origin of Na contamination might have been caused by the cellulose and lignin separation process in which *NaOH aqueous* solutions are usually used [56, 57]. They could be reduced or eliminated by the introduction of certain additional rinsing procedures. The measurements (table 10) show that 2.3% nitrogen is present in the carbon fiber containing Arboform. Based on the carbon fiber in the Arboform matrix, the carbon fiber it self contains almost 10% nitrogen.

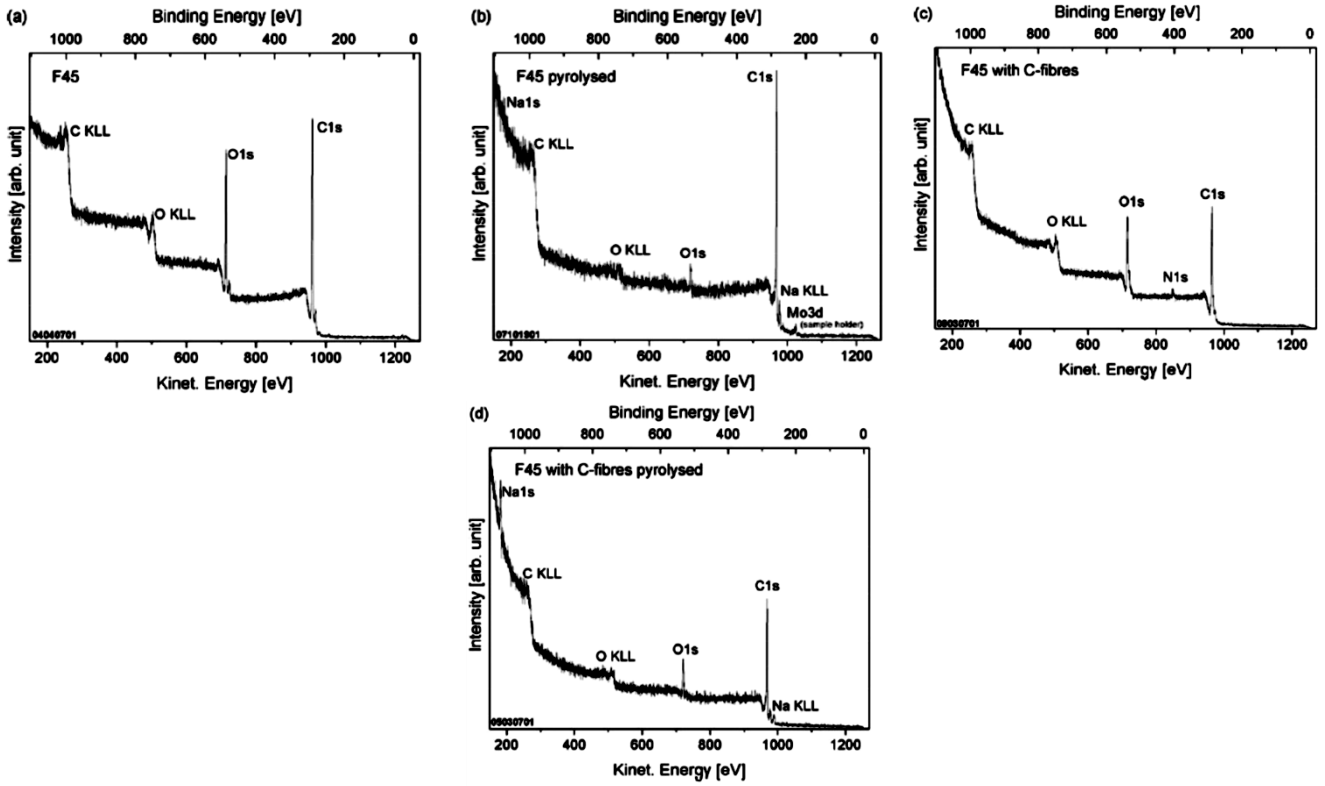

Fig. 32. XPS specter assembly shows contamination on the surface of Arboform F45 (a), pyrolyzed Arboform (b), with C fibers (c) and pyrolysis of C fibers contained by Arboform (d), [44]

Table 10. Relative elementary content of samples, [44]

Sample	C (%)	O (%)	N (%)	Na (%)
F45	84	16	0	0
F45 CF	80.0	17.7	23	0
F45 CF pyr.	88.7	93	0	2
F45 pyr.	94.0	5.7	0	0.3

Traces of Na contamination (<2 la %) is also perceivable; Na contamination is ascribed to the diffusion of contaminants towards surface following pyrolysis. An explanation of Na contamination occurring only following pyrolysis might be that Na is present in minimal quantities in the unpyrolyzed composite polymer that is based on wood, and is below the XPS detection threshold.

The high oxygen content present in the carbon fibers is a result of the process during manufacture. According to Ryu [59] the carbon fibers are subject to oxidation processes to improve interlaminate shear strength. Moreover, Ryu reported that in the case of the carbon fibers with 9.1% nitrogen, based on polyacrylonitrile, the ratio O/C is 0.182. Taking into consideration the above-mentioned information and the fact that in the herein study almost 10% nitrogen is estimated in the carbon fibers, the ratio O/C in the carbon fibers should be roughly the same value. It is widely accepted that a carbon-based material with higher nitrogen content also has higher oxygen content, [59]. From the information above it clearly follows that the reduction of C% in the compound containing the carbon fiber is due to the nitrogen presence and to the fact that the O/C ratio is almost the same for the carbon fibers and wood-based

compound. After pyrolysis the carbon content is lower than in the case of free Arboform with carbon fiber.
A cause may be the higher oxygen content of the raw material. Moreover the greater value of Na (that reacts to oxygen) contamination produces more oxygen in the pyrolyzed carbon fibers containing Arboform (2% Na) than in the free Arboform fibers (0.3% Na). Another cause of the lower carbon content and higher oxygen content following pyrolysis may be ascribed to the thick matrix of the wood-based polymeric compound containing carbon fibers. On the other hand, oxygen cannot be released from the material at the same temperature applied to the system containing onlyArboform F45. Thus it is reasonable that, for the realization of complete pyrolysis, the addition of carbon fibers resulting in thick matrix requires higher temperature. A fine C 1s (figure 33) has been carried out to achieve a detailed analysis of the mandatory sample relative correlations because the peak transition of the functional groups is solvable between different binding correlations, [12]. The peak C-O is moved by 1.4± 0.1 eV and C=O is moved by 3.1 ±0.1 eV at greater binding energy to peak C-C/C-H, in line with the specialty literature, [60, 61].
The binding energy of the lignin-cellulose compound is directed in relation to the carbon fiber signal. Following pyrolysis, the change of basic level energy disappears, which indicates the fact that the fiber compound dissolves in the compound matrix, [44].
Arboform is non-conducting material. As a result, the photoelectrons migrate from the surface and change the surface potential. According to this phenomenon the analyzed basic levels are displaced. Arboform that was not pyrolyzed with C fibers has low conductivity in Arboform matrix and high conductivity across the conducting fiber network. In this event the peaks of the basic levels should be separated in two parts: one representing the matrix and the other component is assigned to the fiber network. This phenomenon is well known in the specialty literature and is called differential loading, [62]. There are a few possibilities to eliminate this phenomenon. One possibility consists in reducing the layer thickness to make it as thin as possible; the thickness reduction has been achieved on wood-based polymers [63], but in this study was not possible. Another possibility is the usage of the neutralizer intended for cellulose [64] and lignin [65] measurements. However, some reports point to the fact that the differential loading may be used to obtain further information on the analyzed material [66, 67]. The basic level satisfies the above presumption and indicates the expected sample composition. Following the pyrolysis at 1200 °C graphitization generates a conducting material. In this case, the differentiation between carbon fiber network and material matrix submitted to pyrolysis is not possible.

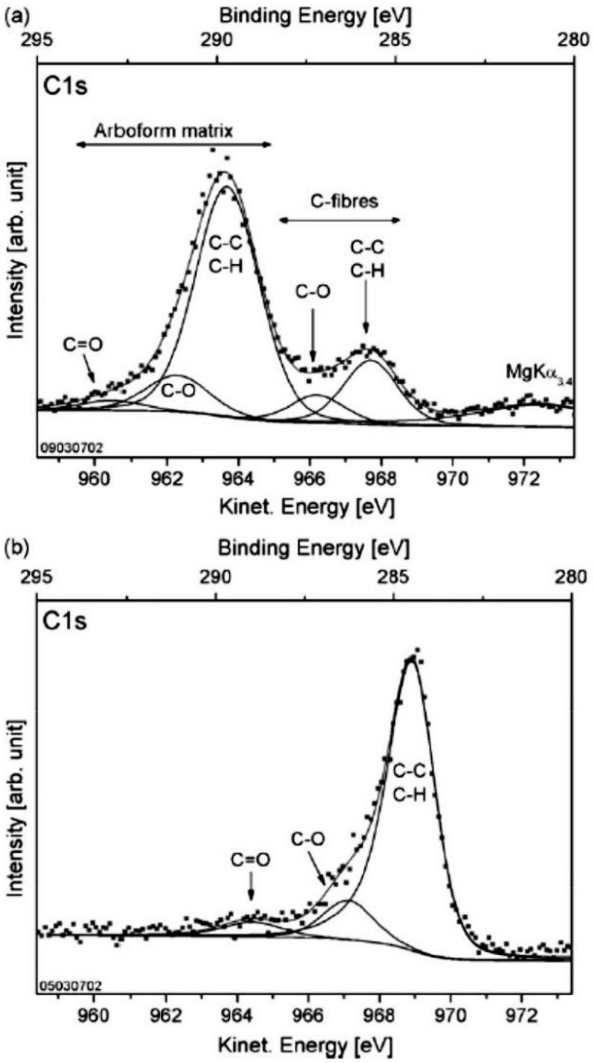

Fig. 33. XPS fine scan of non-pyrolysis (a) and pyrolysis (b) in the carbon fiber containing ArboformF45, [44]

8. FTIR ANALYSIS –FOURIER TRANSFORM INFRARED SPECTROSCOPY

To obtain specters, FTIR Thermo Scientific Nicolet ™ 6700 has been used. Under full regime, the apparatus attenuates total reflection (ATR-IR), has 4 cm^{-1} resolution and can achieve 32 scans per sample.
Figure 34 shows the FTIR specters of the pure PBS, lignin and PBS composite with 50% lignin with and without PMDI. The carbonyl feature (C = O) is present from 1735 to 1750 cm^{-1}, C-O stretches from 1145 to 1155 $cm^{-1}$and C-H stretches from 2850 to 2950cm^{-1} and is evident in PBS specters and its composites. Large hydrogen peaks bind the groups -OH at (3400-3100) cm^{-1}which occur in all lignin specters and composites. The characteristic lignin peaks have been previously discussed in the lignin chapter. It may also be observed that all PBS and lignin characteristic peaks are present in composites. The peak at 1370 cm^{-1}in the lignin specter (due to OH phenol group) moved to 1388 cm^{-1}in the composite specter which might have occurred as a result

of the interaction between lignin OH groups and PBS matrix C = O groups. The NCO (isocyanate) non-characteristic peak, group from 2270 cm^{-1}, occurs in the specters of the compatibilized composites that indicate a complete reaction of the isocyanate in composite system.

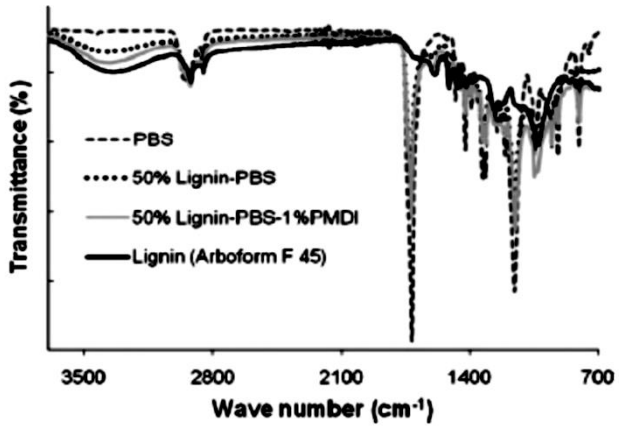

Fig. 34.FTIR specters of lignin, PMDI and composites, [28]

Due to the special properties, Arboform has been extensively used in many fields of activity. Thus this material is used in the automotive industry to make interior parts (fine veneers, panels, battery holder, precise 3D templates, strips, steering wheel) [6, 68, 69, 70], civil engineering (flooring, slabs, hand railing, window frame sections) [6, 71], electronics (spherical loudspeaker, mobile case and cover, loudspeaker board, keyboard, mouse) [6, 21,72, 73], commodities industries (knives, glasses, plates, glass pads, films) [6, 74, 75]), precision mechanics (watch cases, sporting riffle, technical parts) [6, 18, 76], furniture industry (chairs, armchairs arms, table legs) [6, 70], manufacture of musical instruments (flute, harmonica) [73], jewelry (jewelry box, pendant, beads) [2], toys (baby- pacifier, play board, nativity figurine) [2], gardening products (garden furniture, garden implements) [6], and other general interest products (heels and shoe platform, stamps, vase, lamps, ornamental spheres, hangers, eyeglasses frames, funerary urns, small-sized coffins) [75].

9. CONCLUSIONS

"Liquid wood" is available in three different types such as: ARBOFORM ¯ Liquid wood (based on lignin, organic additives and natural fibers), ARBOBLEND plastic composite with wood (its content is based on biopolymers degree, e.g.: lignin, starch, natural resins, wax and cellulose), ARBOFILL biopolymeric composite (polymers and natural fibres-based compound provided with natural cork aspect).
The Arboform has been developed by Fraunhofer Institute for Chemical Technology together with Tecnaro GmbH, Germany. Arboform is available in three product variants according to the corresponding quantities of mixed components: LV3 Nature, F45Nature and LV5 Nature.
Take into account all the researches presented in this article the Arboform is the material that will replace plastic in the near future. Considering the results presented, mechanical, thermal, chemical, electrical, structural properties, the following plastic materials could be replaced: PE (polyethylene), PVDF (Poly Vinylidene Fluoride), PCTFE (Ethylene Copolymer) PA 12 (polyamide); PE-HD (High Density Polyethylene); ABS (Acrylonitrile-butadiene-styrene); PVDF (Poly Vinylidene Fluoride), ECTFE (Etylene Copolymer); POM (Acetal Homopolymer) etc. Also it is important to pint out that the Arboform can be reinforced with different natural fibers leading to the injection process improvement and increase of properties.

ACKNOWLEDGMENT

This work was supported by the strategic grant POSDRU/159/1.5/S/133652, co-financed by the European Social Fund within the Sectorial Operational Program Human Resources Development 2007 – 2013.

10. REFERENCES

1.Srikanth Pilla, (2011), *Engineering Applications of Bioplastics and Biocomposites- An overview*, Handbook of Bioplastics and Biocomposites Engineering Applications, Published John Wiley & Sons, New Jersey,pp. 1-14.
2.Helmut Nagele, Jurgen Pfitzer, Lars Ziegler, Emilia Regina Inone-Kauffmann, Wilhelm Eckl, and Norbert Eisenreich, (2014), *Lignin Matrix Composites from Natural Resources - ARBOFORM®, Bio-Based Plastics: Materials and Applications*, First Edition. Edited by Stephan Kabasci, John Wiley &Sons.Ltd. Published 2014 by John Wiley & Sons, Ltd.
3.Laurichesse S, Av´erous L, (2013), *Chemical modification lignins: towards biobased polymers*, Progress in Polymer Science (2013), http://dx.doi.org/10.1016/j. progpolymsci..11.004.
4.Patanjali Varanasi, Priyanka Singh, Manfred Auer, Paul D Adams, Blake A SimmonsandSeema Singh, (2013), Survey of renewable chemicals produced from lignocellulosic biomass during ionic liquid pretreatment,Biotechnology for Biofuels.
5.International Lignin Institute: http://www.ili-lignin.com/aboutlignin.php Accessed at: 12.02.2014.
6.Official Arboform producer webpage: http://www.tecnaro.de/english/grundsaetze.htm?section=arboform Accessed at: 10.02.2014.
7.Jae-Young Kim, Eun-Jin Shin, In-Yong Eom, Keehoon Won, Yong Hwan Kim , Donha Choi ,In-Gyu Choi, JoonWeon Choi, (2011), *Structural features of lignin macromolecules extracted with ionic liquid from poplar wood*, Bioresource Technology 102, pp. 9020–9025.

8.Oldham, P.B., Wang, J., Conners, T.E. and Schultz, T.P. (1993) *Rapid analysis of pulp lignin: a review of N1R and FTIR and preliminary investigation of multidimensional fluorescence spectroscopy*. Pulping Conference, pp. 653.
9.Porter, J., Sands, T. and Trung, T. (2009) *Understanding Kraft liquor cycle: a need for online measurement and control.* TAPPI Engineering, Pulping and Environmental Conference October 11-14, Memphis Tennessee, pp. 1-12.
10.Becker W., Inone-Kauffmann E., Eckl W., Eisenreich N., (2007), *Near infrared spectroscopy for inline control of biopolymer Processing*. Proceedings of the Polymer Processing Society, Annual Meeting, PPS23, San Salvador, Brazil.
11.Rohe T., Becker W.,Krey A. et al. (1998), *In-line monitoring of polymer extrusion processes by NIR spectroscopy*, Journal of Near Infrared Spectroscopy, 6, 325-332.
12.Martens, H. and Naes, T., (1989), *Multivariate Calibration*, John Wiley & Sons, Ltd, Chichester.
13.Jedicke, O.Eisenreich, N. and Diimpert, H., (2000), *Aquasolv® - Hydrothermolyse -The Development of a Process for Completely Use of Biomass*, Proceedings 1st Biomass World Conference, Sevilla, Spain.
14.Practical research of wood-like thermoplastic using lignin extracted by high pressure hydrolysis process, (Patent registration number 2002GP008).
15.Mohanty, A. K., Misra, M. and Drzal, L. T., (2002), *Sustainable Bio-Composites from Renewable Resources: Opportunities and Challenges in the Green Materials World*, Journal of Polymers and the Environment, 10(1/2).
16.Naegele H., Pfitzer J., Naegele E., Inone ER., Eisenreich N., Eckl W., et al. (2002), *ARBOFORM – a thermoplastic, processable material from lignin and natural fibers*. In: Hu TQ, editor. Chemical modification, properties, and usage of lignin, New York, Kluwer Academic/Plenum.
17.Dumitru Nedelcu, Ciprian Ciofu, Nicoleta Monica Lohan, (2013), *Microindentation and differential scanning calorimetry of ''liquid wood''*, Composites: Part B 55, pp. 11–15.
19.Ellis, Meagan, (2009), *Toy turn for bioplastics*, *Materials World*, 17(2), ProQuestCentral, pp. 20.
20.Mark Johnson, (2004), *Commercially Available Low Environmental Impact Polymers*, Low Environmental Impact Polymers: Overview.
21.Nägele, H., Pfitzer, J., Lehnberge,r C., Landeck, H., (2005), *Renewable resources for use in printed circuit boards*, Circuit World; 31, 2, ProQuest Central, pp. 26.
22."How Arboform Works" How Stuff Works. [Online: Blog]. Available: http://blogs.howstuffworks.com/ 2010/07/19/how-arboform-works-a-plastic-made-of-lignin-from-wood-that-biodegrades-like-wood/, (2011).
23.Björn Winberg, KAM Industries, (2010), *Albis Plastic Scandinavia AB*, Commercial biopolymers Properties and limitations.
24."Liquid Wood: A New Plastic That Grows on Trees" Discover Magazine. [Online: Article]. Available: http://blogs.discovermagazine.com/ discoblog/2008/12/04/liquid-wood-a-new-plastic-that-grows-on-trees/, (2011).
25."A Greener Alternative to Plastics: Liquid Wood" MSNBC. [Online; Article]. Available. http://www.msnbc. msn.com/id/28283260/ns/technology_ and_science-innovation/t/greener-alternative-plastics-liquid-wood/#.Tq9R3VZkedx, (2008).
26.A batter world "liquid wood": Eco-friendly alternative to synthetic plastics. Available. http://www.youthxchange.net/main/ai136_liquid-wood.asp, Accessed at 12.03.2014.
27.Jürgen Pfitzer, Helmut Nägele, (2011), *Trends beiBiokunststoffen – Anwendungsbeispiele und Neuentwicklungen*, Tecnaro GmbH.
28.Saswata Sahoo, Manjusri Misra, Amar K. Mohanty, (2011), *Enhanced properties of lignin-based biodegradable polymer composites using injection moulding process*, Composites: Part A 42: 1710–1718.
29.Toriz G, Denes F, Young RA, (2002), *Lignin-polypropylene composites. Part1: composites from unmodified lignin and polypropylene*. Polym Compos; 23: pp. 806–13.
30.Nyambo C, Mohanty AK, Misra M., (2010), *Polylactide-based renewable greencomposites from agricultural residues and their hybrids*, Biomacromolecules; 11: pp. 1654–60.
31.Kim HS, Yang HS, Kim HJ., (2005), *Biodegradability and mechanical properties of agroflour–filled polybutylene succinate biocomposites*, J Appl Polym Sci; 97:1513–21.
32.Jiang L, Chen F, Qian J, Huang J, Wolcott M, Liu L, et al. (2010), *Reinforcing andtoughening effects of bamboo pulp fibre on poly (3-hydroxybutyrate-co-3-hydroxyvalerate) fibre composites*, Ind Eng Chem Res; 49:572–7.
33.Ciemniecki SL, Glasser WG. (1989), *Polymer blends with hydroxypropyl lignin*. In: Glasser WG, Sarkanen S, editors. Lignin properties and material. Washington (DC): American Chemical Society.
34.Chen F, Liu L, Cooke PH, Hicks KB, Zhang J. (2008), *Performance enhancement of poly (lactic acid) and sugar beet pulp composites by improving interfacial adhesionand penetration*. Ind Eng Chem Res; 47:8667–75.
35.Madden JP, Baker GK, Smith CH. (1971), *Study of polyether-polyol- and polyesterpolyol-based rigid urethane foam systems.* In: Technical report made for United States department of energy and paper submitted to 162nd national meeting. Washington, DC: American Chemical Society, September.
36.Shih YF, Lee WC, Jeng RJ, Huang CM, (2006), *Water bamboo husk-reinforcedpoly (butylene succinate) bio-degradable composites.* J Appl Polym Sci; 99:188–99.

37.Scholz G, Lohr J, Windeisen E, Tröger F, Wegener G. (2009), *Carbonization of hotpressedArboform-mixtures*. Eur J Wood Wood Prod; 67:351–5.
38.Lee SM, Cho D, Park WH, Lee SG, Han SO, Drzal LT. (2005), *Novel silk/poly (butylene succinate) biocomposites: the effect of short fibre content on their mechanical and thermal properties*. Compos Sci Technol; 65:647–574.
39.Lee B-H, Kim H-S, Lee S, Kim H-J, Dorgan JR, (2009), *Bio-composites of kenaf fibers inpolylactide: role of improved interfacial adhesion in the carding process*.Compos Sci Technol;69:2573–9.
40.Singh S, Mohanty AK, Sugie T, Takai Y, Hamada H. (2008), *Renewable resource basedbiocomposites from natural fiber and polyhydroxybutyrate-co-valerate (PHBV) bioplastic*. Composites: Part A, 39,:875–86.
41.Jordan, J. Jacob, K.I., Tannenbaum, R. et al. (2005), *Experimental trends in polymer nanocomposites - a review*. Materials Science and Engineering A, 393, 1-11.
42.Droval, G., Feller, J.F., Salagnac, P. and Glouannec, P. (2008*), Conductive polymer composites with double percolated architecture of carbon nanoparlicles and ceramic microparticles for high heat dissipation and sharp PTC switching*, Smart Materials and Structures, 17 (2), 1-10.
43.Devi G., Rao V.J., (2000), *Room temperature synthesis of colloidal platinum nanoparticles*, Bulletin of Materials Science, 23, 467-470.
44.Thomas Haensel, Andreas Comouth, Nicolas Zydziak, Eva Bosch, Axel Kauffmann, Juergen Pfitzer, Stefan Krischok, Juergen A. Schaefer, Syed Imad-Uddin Ahmeda, (2010), *Pyrolysis of wood-based polymer compounds*, Journal of Analytical and Applied Pyrolysis, 87, pp.124–128.
45.M. Filippi, L. Calliari, (2006), Surf. Interf. Anal., 38, pp. 595.
46.E. Camps, L. Escobar-Alarco´n, M.E. Espinoza, M.A. Camacho-Lo´ pez, S.E. Rodil, S.Muhl, (2003), *Superficies Vacio*, 16, pp. 37.
47.Kauffmann, A., Eisenreich, N., Weiser, V., (2005), *LeitfahigesFormteil, Verfahrenzu seiner Herstel-lung und Verwendungdesselben*, DE 103 47 701 Al.
48.Hadjiev, H., Frey, H., Khan. H.R. (2011), *Decompositon and oxidation of cyclopentasilane diluted in toluene*. Proceeding of 42nd International Annual Conference of Fraunhofer ICT, Karlsruhe, Germany. June-01 July, p. 103.
49.Hadjiev, H., Khan, H.R., Frey, H. et al. (2012) *Decomposition and oxidation of cyclopentasilane*. Proceeding of 43rd International Annual Conference, of the Fraunhofer ICT, Karlsruhe, Germany, 26 June - June.
50.H. Naegele, J. Pfitzer, C. Lehnberger, H. Landeck, K. Birkner, U. Viebahn, W. Scheel,R. Schmidt, M. Hagenlken, J. Mller, (2005), *Circuit World*, 31, pp.26.
51.http://www.tohotenax-eu.com/. Accessed at 12.11.2013.
52.R. Taipalus, T. Harmia, M.Q. Zhang, K. Friedrich, (2001), Compos. Sci. Technol. 61 801.
53.G. Cherkashinin, S. Krischok, M. Himmerlich, O. Ambacher, J.A. Schaefer, (2006), J. Phys.Condens. Matter 18, 9841.
54.Weihua K, He Y, Asakawa N, Inoue Y. (2004) ,Effect of lignin particles as a nucleating agent on crystallization poly (3-hydroxybutyrate). J Appl Polym Sci; 94: 2466–74.
55.J.J. Yeh, I. Lindau, At. Data Nucl. Data Table 32 (1985) 1.
56.A. Isogai, R.H. Atalla, Cellulose 5 (1998) 309.
57.H.M. Wang, R. Postle, R.W. Kessler, W. Kessler, (2003), Text. Res. J., 73, 664.
58.S.-K. Ryu, B.-J. Park, S.-J. Park, (1999), J. Colloid Interf. Sci., 215, 167.
59.E. Pollak, G. Salitra, A. Soffer, D. Aurbach, (2006), Carbon, 44, 3302.
60.G. Beamson, D. Briggs, (1998), *The XPS of Polymers Database*, Surface Spectra, Manchester,.
61.L.M. Matuana, J.J. Balatinecz, R.N.S. Sodhi, C.B. Park, (2001), Wood Sci. Technol., 35, 191.
62.R.H. Bradley, I.L. Clackson, D.E. Sykes, (1994), Surf. Interf. Anal., 22, 497.
63.L. Klarho¨ fer, B. Roos, W. Vio¨ l, O. Ho¨ fft, S. Dieckhoff, V. Kempter, W. Maus-Friedrichs, Holzforschung 62 (2008), 688.
64.L.-S. Johansson, Mikrochim. Acta 138 (2002) 217.
65.T. Haensel, A. Comouth, P. Lorenz, S.I.-U. Ahmed, S. Krischok, N. Zydziak, A.Kauffmann, J.A. Schaefer, (2009), Appl. Surf. Sci. 255, 8183.
66.F. Karadas, G. Ertas, S. Suzer, (2004), J. Phys. Chem. B 108, 1515.
67.M. Dubey, I. Gouzman, S.L. Bernasek, J. Schwartz, Langmuir 22 (2006) 4649.
68.http://land-der-erfinder.de/?tag=arboform, Accessed at: 16.03.2014.
69.http://www.gruene-wunstorf.com/themen /allgemein-von-a-z/abfallwirtschaft/agrarwende/ bildung-allgemein/b%C3%BCrgerbeteiligung/city-bike/fracking/fukushima-mahnt/gigaliner/mox/ plastik-aus-holz/, Accessed at: 16.03.2014
70.http://www.greendiary.com/liquid-wood.html, Accessed at: 15.02.2014.
71.http://www.besedki.ck.ua/news/uchenye_izobreli_zhidkuju_drevesinu/2012-11-18-11, Accessed at: 12.03.2014.
72.http://norskmand.com/portfolio/liquid-wood-iphone-5-flap-case/, Accessed at: 16.03.2014.
73.http://www.plasticstoday.com/mpw/articles/fujitsu-launches-injection-molded-bioplastic-keyboard, Accessed at: 10.03.2014.
74.http://www.behance.net/gallery/Starbucks-Arboform-Cup/14089743, Accessed at: 16.03.2014.
75.http://aesop-innovation.com/pages/liquidwood-news.php, Accessed at: 15.03.2014.
76.http://www.designinsite.dk/htmsider/k0076.htm, Accessed at: 16.03.2014.

Received: April 15, 2014 / Accepted: December 10, 2014 / Paper available online: December 15, 2014 © International Journal of Modern Manufacturing Technologies.